

# Extensions of Random Orthogonal Matrix Simulation for Targetting Kollo Skewness

Carol Alexander\* Xiaochun Meng<sup>†</sup> Wei Wei<sup>‡</sup>

## Abstract

Multivariate systems have ubiquitous applications to many problems that are commonly resolved using simulation methods, especially when the distributions under scrutiny have no closed form and the system has many dimensions. Random Orthogonal Matrix (ROM) simulation is a method that has gained some popularity in this context because certain simulation errors are removed. Specifically, it *exactly* matches a target mean, covariance matrix and certain higher moments in every simulation. This paper extends and modifies the ROM simulation algorithm presented by Hanke et al. (2017), hereafter referred to as HPSW, which extends the original algorithm of Ledermann et al. (2011) to match Kollo skewness exactly. Our first contribution is to establish necessary and sufficient conditions for the HPSW algorithm to work. Then we introduce two novel methods for speeding up the algorithm and improving the statistical properties of each simulated marginal distribution. Another theoretical result, this time on multivariate sample concatenation, shows how to improve the sequential dynamics of ROM simulated data. Finally, we apply the extended and modified HPSW algorithm to real-world data and illustrate our theoretical results with some extensive numerical analysis.

**Keywords:** Simulation; Algebraic statistics, L matrices, Multivariate skewness, ROM simulation

**JEL Codes:** C15, C63.

---

\*Corresponding author. University of Sussex Business School and Peking University PHBS Business School. Email: c.alexander@sussex.ac.uk

<sup>†</sup>University of Sussex Business School. Email: xiaochun.meng@sussex.ac.uk.

<sup>‡</sup>University of Sussex Business School. Email: wei.wei@sussex.ac.uk.

# 1 Introduction

Modelling multivariate systems is important for many applications in operational research but also in economics, engineering, environmental science, finance, medicine and other disciplines that require quantitative analysis. In the vast majority of cases, the multivariate distributions under scrutiny have no analytic or closed form, so the problem can only be resolved using some type of numerical technique. Of these, Monte Carlo (MC) simulation is most commonly used because it is fast, the basic method is quite straightforward and the random samples generated converge to the distribution in probability (Thomopoulos, 2012). However, the sample moments are not equal to their population values and even when the experimenter performs a very large number of simulations the differences can be considerable. As a result, sampling error and uncertainty in MC methods have been widely studied (see, for example, Oberkampf et al. 2002 and Ferraz and Moura 2012). For this reason, much research focusses on developing variance-reduction techniques aimed at improving the efficiency of simulations – see, for example, Swain and Schmeiser (1988), Hesterberg (1996), Szántai (2000), Saliby and Paul (2009) and many others. These have applications to any problem which requires the use of multivariate simulations for its resolution. For instance, see Badano and Samuelson (2013) and Quintana et al. (2015) for multivariate simulations used in engineering applications, and Avramidis and Matzinger (2002), Capriotti (2008), and Ma and He (2016) for problems in finance.

Addressing the simulation error problem from a different perspective entirely, Ledermann et al. (2011) introduces a novel and flexible method for generating random samples from a correlated, multivariate system called Random Orthogonal Matrix (ROM) simulation. It is based on the premise of *exactly* matching a target mean, covariance matrix and certain higher moments with *every* simulation. Several developments have extended the original paper, for instance, Ledermann and Alexander (2012) investigate the effect of different random rotation matrices on ROM simulation sample characteristics. And Hürlimann (2013) presents a very significant theoretical development of ROM simulation by extending the basic  $L$  matrices (which are fundamental to ROM simulation, as we shall see below) to a much broader class of generalised Helmert-Ledermann (GHL) matrices, thereby increasing flexibility and scope of ROM simulation.

ROM simulation has already been applied in a variety of real-world applications. For instance, Geyer et al. (2014) implements ROM simulation in an arbitrage-free setting, for option pricing and hedging. Hürlimann (2014) integrates ROM simulation into two semi-parametric methods that take into account skewness and kurtosis, in order to improve the computation of quantiles for linear combinations of the system variables, and Alexander and Ledermann (2012) investigate the use of target skewness and kurtosis via ROM simulation for stress testing.

Further theoretical developments focus on the higher-moment characteristics of ROM simulation: Hürlimann (2015) introduces a new, recursive method for targetting the skewness and kurtosis metrics of Mardia (1970) using ROM simulation with GHL matrices, and Hanke et al. (2017) improve on the skewness metric that ROM simulation can target, using the vector-valued moment of Kollo (2008) in place of the Mardia skewness.

This paper extends and modifies the algorithm presented by Hanke et al. (2017) – hereafter referred to as HPSW. First, on testing its implementation we found that the HPSW algorithm does

not always work. This is because the algorithm requires selecting many so-called ‘arbitrary’ real values but we found that some values are inadmissible because they yield complex-valued roots for the equations that must be solved. This problem becomes more and more prevalent as the dimension of the system increases. We therefore derive necessary and sufficient conditions for the HPSW algorithm to work, i.e. for the existence of real roots of the HPSW equations. When real roots do exist we call the arbitrary values “admissible”.

It is easier to find admissible arbitrary values when they have low variance. In fact, the code provided with Hanke et al. (2017) sets to zero, all arbitrary values for the first variable of the (rotated) system, and the arbitrary values for all other variables are independently drawn from a standard uniform distribution. We show that, this way, the zero arbitrary values are (almost) always admissible but there can be a relatively high failure rate for the algorithm because the other arbitrary values are too variable. Moreover, the simulations that can be generated this way have long periods of zero or minimal activity interspersed with periods of high activity. This could be a very useful feature for applications to climate modelling or medical research – for instance, such patterns are commonly observed in multivariate seismic wave dynamics (Takanami and Kitagawa 1991, Adelfio et al. 2012 and others) and cardiology (see McSharry et al. 2003, Lyon et al. 2018 and others). However, such extreme patterns have little relevance to problems in economics and finance, for instance.

Our second contribution is to modify the algorithm with two novel methods for constructing admissible values, based on bootstrapping and parametric distributions. We analyse the maximum variability that is admissible and apply our results to some real data. The features of our modified HPSW algorithm are ideally suited to modelling financial systems, where heteroscedasticity is common (see Engle 1982, Bollerslev et al. 1994 and a highly prolific theoretical and applied literature since then). This is because the targeted moments are captured entirely by the periods of high activity, with arbitrary values filling in the ‘unstressed’ or ‘normal’ market condition. Our third theoretical contribution is to extend the HPSW algorithm to include multivariate sample concatenation, providing sufficient conditions for the target Kollo skewness to be invariant and thereby generalising the covariance results of Ledermann et al. (2011). All code is available from the authors on request.

The extensions of the HPSW algorithm that we develop in this paper should increase the scope of ROM simulation to reflect characteristics of real-world applications, especially in large systems. The paper ends with an empirical study using two multivariate systems of financial asset returns, and presents some numerical results based on an assumed parametric distribution. In the following: Section 2 fixes notation and concepts; Section 3 extends the developments of ROM simulation proposed by Hanke et al. (2017) with: necessary and sufficient conditions for the selection of admissible values in their algorithm; thereby proposing novel methods for generating such values; and motivating the use of sample concatenation and analysing its effect on target Kollo skewness; Section 4 provides our empirical results and Section 5 concludes. All theoretical results are proved in Appendix A.

## 2 Background

In this section we fix notation by providing a brief overview of the basic concepts for both ROM simulation and multivariate skewness. The first subsection summarises the initial development of ROM simulation by Ledermann et al. (2011) and Ledermann and Alexander (2012) who target the mean vector and the covariance matrix, and the second subsection reviews the work of Hanke et al. (2017) which also targets skewness. Specifically, every simulation is specifically designed to have exactly the same mean, covariance matrix and Kollo skewness vector.

### 2.1 ROM Simulation

Suppose we want to simulate from an  $n$ -dimensional random variable with mean vector  $\boldsymbol{\mu}_n$ , and covariance matrix  $\mathbf{V}_n$ . Let  $\mathbf{X}_{mn}$  denote the  $m \times n$  matrix of simulations, where  $m$  denotes the number of observations. In order to match the mean and covariance of the samples  $\mathbf{X}_{mn}$  with  $\boldsymbol{\mu}_n$  and  $\mathbf{V}_n$ , the following equations must be satisfied:

$$m^{-1} \mathbf{1}'_m \mathbf{X}_{mn} = \boldsymbol{\mu}'_n, \quad (1)$$

$$m^{-1} (\mathbf{X}'_{mn} - \mathbf{1}_m \boldsymbol{\mu}'_n) (\mathbf{X}_{mn} - \mathbf{1}_m \boldsymbol{\mu}'_n) = \mathbf{V}_n, \quad (2)$$

where  $\mathbf{1}_m$  is a column vector with all ones and  $'$  denotes the matrix transpose. Ledermann et al. (2011) show that (1) and (2) hold if and only if  $\mathbf{X}_{mn}$  takes the following form:

$$\mathbf{X}_{mn} = \mathbf{1}_m \boldsymbol{\mu}'_n + m^{1/2} \mathbf{Q}_m \mathbf{L}_{mn} \mathbf{R}_n \mathbf{A}_n, \quad (3)$$

$$\mathbf{L}'_{mn} \mathbf{L}_{mn} = \mathbf{I}_n, \quad (4)$$

$$\mathbf{1}'_m \mathbf{L}_{mn} = \mathbf{0}'_n, \quad (5)$$

where  $\mathbf{0}_n$  is the column vector with all zeros,  $\mathbf{I}_n$  is the identity matrix,  $\mathbf{V}_n = \mathbf{A}'_n \mathbf{A}_n$  and both  $\mathbf{Q}_m$  and  $\mathbf{R}_n$  are orthogonal matrices. In ROM simulation,  $\mathbf{Q}_m$  is a random permutation matrix which functions to re-order the observations;  $\mathbf{R}_n$  is a random rotation matrix which can re-generate  $\mathbf{X}_{mn}$  by simply changing  $\mathbf{R}_n$ , and the matrix  $\mathbf{L}_{mn}$  is taken from a class of rectangular orthogonal matrices known as  $L$  matrices. In equation (3), the sample mean and covariance of  $\mathbf{X}_{mn}$  are determined solely by  $\boldsymbol{\mu}_n$  and  $\mathbf{A}_n$ , given that  $\mathbf{L}_{mn}$  satisfies equations (4) and (5). Hence,  $L$  matrices are a cornerstone of ROM simulation and to generate  $\mathbf{X}_{mn}$  we need firstly obtain a  $L$  matrix.

In addition to the ability to match the exact mean and covariance matrix, ROM simulation is generally much faster than MC simulation, especially in high-dimensional systems, because samples are generated by simply changing  $\mathbf{R}_n$  to another random rotation matrix and performing the required matrix multiplications. See Ledermann and Alexander (2012) for the classification of different types of rotation matrix and their effects on ROM simulation sample characteristics.

## 2.2 ROM Simulation with Target Kollo Skewness

This section summarises the ROM simulation approach proposed by Hanke et al. (2017) to target mean vector, covariance matrix, and Kollo skewness vector. Consider a correlated system of  $n$  random variables  $\mathbf{Y}_n = [Y_1, Y_2, \dots, Y_n]$  having mean  $\boldsymbol{\mu}_n$  and covariance matrix  $\mathbf{V}_n$  and use the notation  $\mathbf{Y}_n^*$  for the standardised versions of  $\mathbf{Y}_n$ , i.e.

$$\mathbf{Y}_n^* = (\mathbf{Y}_n - \mathbf{1}_m \boldsymbol{\mu}_n') \mathbf{V}_n^{-1/2}.$$

A typical way to define the skewness of their multivariate distribution is to set  $c_{ijk} = \mathbb{E}[Y_i^* Y_j^* Y_k^*]$  for each tuple  $(Y_i^*, Y_j^*, Y_k^*)$ , with  $i, j, k = 1, \dots, n$ . Then, for each  $i = 1, \dots, n$ , form the matrix

$$\mathbf{C}_i = \begin{bmatrix} c_{i11} & c_{i12} & \cdots & c_{i1n} \\ \vdots & \vdots & \ddots & \vdots \\ c_{in1} & c_{in2} & \cdots & c_{inn} \end{bmatrix},$$

and finally define the *co-skewness tensor* as:

$$\mathbf{m}_3 = [\mathbf{C}_1, \mathbf{C}_2, \dots, \mathbf{C}_n]. \quad (6)$$

The co-skewness tensor has good properties such as invariance under affine, non-singular transformations (Mardia, 1970). However,  $\mathbf{m}_3$  has  $n^3$  elements which makes it impractical for use in large systems, hence the need to construct summary skewness metrics.

Mardia (1970) proposes multivariate skewness as follows:

$$\beta_1(\mathbf{Y}_n) = \sum_{i,j,k=1}^n c_{ijk}^2. \quad (7)$$

It can be shown that Mardia skewness is essentially the sum of all the squared elements in (6). However, Gutjahr et al. (1999) show that, being a simple scalar, the Mardia skewness loses much of the information contained in the co-skewness tensor (6). This motivates Hanke et al. (2017) to focus on the skewness measure proposed by Kollo (2008), which is a  $n$ -dimensional vector with  $i^{\text{th}}$  element equal to the sum of the elements of the  $i$ -th row in equation (6), i.e.:

$$\boldsymbol{\tau}(\mathbf{Y}_n) = \left[ \sum_{i,k}^n c_{i1k}, \sum_{i,k}^n c_{i2k}, \dots, \sum_{i,k}^n c_{ink} \right]'. \quad (8)$$

Let  $\boldsymbol{\mu}_n$ ,  $\mathbf{V}_n$  and  $\boldsymbol{\tau}_n$  be the target mean vector, covariance matrix, and Kollo skewness vector that we want to match. Equations (3) – (5) only guarantee that  $\mathbf{X}_{mn}$  matches the target mean and covariance, but it remains to match Kollo skewness which can be affected by  $\mathbf{L}_{mn}$  and  $\mathbf{R}_n$ . So the problem is to find a suitable  $\mathbf{L}_{mn} \mathbf{R}_n$  such that  $\mathbf{X}_{mn}$  can match the Kollo skewness. For convenience, Hanke et al. (2017) work with a scaled  $L$  matrix defined by  $\mathbf{M}_{mn} = m^{1/2} \mathbf{L}_{mn} \mathbf{R}_n$  so that equation (3) can be written:

$$\mathbf{X}_{mn} = \mathbf{1}_m \boldsymbol{\mu}_n' + \mathbf{Q}_m \mathbf{M}_{mn} \mathbf{A}_n. \quad (9)$$

As a consequence, Hanke et al. (2017)'s algorithm (The HPSW algorithm) is to find a scaled  $L$  matrix  $\mathbf{M}_{mn}$  and further obtain  $\mathbf{X}_{mn}$  by equation (9). According to the definition, is easy to write the sample Kollo skewness for  $\mathbf{X}_{mn}$  as:

$$\boldsymbol{\tau}(\mathbf{X}_{mn}) = m^{-1} \sum_{i=1}^m \alpha_i \mathbf{r}'_i, \quad (10)$$

where  $\mathbf{r}_i$  is the  $i$ -th row of  $\mathbf{M}_{mn}$  and  $\alpha_i = (\mathbf{r}_i \mathbf{1}_n)^2$ ,  $i = 1, \dots, m$ . To solve the equations  $\boldsymbol{\tau}(\mathbf{X}_{mn}) = \boldsymbol{\tau}_n$  for some target Kollo skewness vector  $\boldsymbol{\tau}_n$  and it proceeds as follows: Set

$$\mathbf{S}_{mn} = \mathbf{M}_{mn} \boldsymbol{\Omega}_n = m^{1/2} \mathbf{L}_{mn} \mathbf{R}_n \boldsymbol{\Omega}_n, \quad (11)$$

where  $\boldsymbol{\Omega}_n$  is any orthogonal rotation matrix whose first column is  $n^{-1/2} \mathbf{1}_n$  having the property that

$$\mathbf{1}'_n \boldsymbol{\Omega}_n = n^{1/2} [1, 0, \dots, 0].$$

Let  $\mathbf{s}_i$  be the  $i$ -th row of  $\mathbf{S}_{mn}$ ,  $i = 1, \dots, m$ , i.e.  $\mathbf{s}_i = \mathbf{r}_i \boldsymbol{\Omega}_n$  (and  $\mathbf{s}_i \boldsymbol{\Omega}'_n = \mathbf{r}_i$  because  $\boldsymbol{\Omega}_n$  is orthogonal). Then the equation  $\boldsymbol{\tau}(\mathbf{X}_{mn}) = \boldsymbol{\tau}_n$  may be written:

$$\boldsymbol{\tau}_n = m^{-1} \sum_{i=1}^m (\mathbf{r}_i \mathbf{1}_n)^2 \mathbf{r}'_i = m^{-1} \sum_{i=1}^m (\mathbf{s}_i \boldsymbol{\Omega}'_n \mathbf{1}_n)^2 \boldsymbol{\Omega}_n \mathbf{s}'_i = m^{-1} n \boldsymbol{\Omega}_n \sum_{i=1}^m s_{i1}^2 \mathbf{s}'_i. \quad (12)$$

Next, pre-multiply the matrix  $n^{-1} \boldsymbol{\Omega}'_n$  on both sides of equation (12) and set the vector, it becomes:

$$\mathbf{p}_n = m^{-1} \sum_{i=1}^m s_{i1}^2 \mathbf{s}'_i, \quad (\text{Exact Kollo skewness}) \quad (13)$$

where  $\mathbf{p}_n = n^{-1} \boldsymbol{\Omega}'_n \boldsymbol{\tau}_n$ . Noted that the first element of  $\mathbf{p}_n$  always has  $p_1 = n^{-3/2} \mathbf{1}'_n \boldsymbol{\tau}_n$ . In addition, because  $\mathbf{M}_{mn}$  is a scaled  $L$  matrix,  $\mathbf{S}_{mn}$  must satisfy:

$$\mathbf{S}'_{mn} \mathbf{S}_{mn} = m \mathbf{I}_n, \quad (\text{Exact covariance matrix}) \quad (14)$$

$$\mathbf{1}'_m \mathbf{S}_{mn} = \mathbf{0}'_n. \quad (\text{Column sum constraint}) \quad (15)$$

Hence, we should first generate  $\mathbf{S}_{mn}$  to satisfy equations (13) – (15) and then set:

$$\mathbf{X}_{mn} = \mathbf{1}_m \boldsymbol{\mu}'_n + \mathbf{Q}_m \mathbf{S}_{mn} \boldsymbol{\Omega}'_n \mathbf{A}_n \quad (16)$$

For convenience, let  $s_{1k}, \dots, s_{mk}$  denote the elements in the  $k$ -th column of  $\mathbf{S}_{mn}$  and  $p_k$  denote the

$k$ -th element of  $\mathbf{p}_n$ . With this notation, for each column  $k$ , we rewrite equations (13) – (15) as:

$$m^{-1} \sum_{i=1}^m (s_{i1})^2 s_{ik} = p_k, \quad (\text{Exact Kollo skewness}) \quad (17-1)$$

$$m^{-1} \sum_{i=1}^m s_{ik}^2 = 1, \quad (\text{Exact covariance matrix 1}) \quad (17-2)$$

$$\sum_{i=1}^m s_{ik} s_{ij} = 0, \quad j < k, \quad (\text{Exact covariance matrix 2}) \quad (17-3)$$

$$\sum_{i=1}^m s_{ik} = 0. \quad (\text{Column sum constraint}) \quad (17-4)$$

The HPSW algorithm solves equations (17-1) to (17-4) sequentially, from  $k = 1$  to  $k = n$ . However, there are  $m$  unknown variables in each column but there are only  $k+2$  constraints in the  $k^{\text{th}}$  column. For example, for  $k = 1$  the  $m$  unknowns are  $s_{11}, s_{21}, \dots, s_{m1}$ , but there are only 3 constraints. Hanke et al. (2017) address this under-determinacy by prescribing arbitrary values  $w_{ik}$  to some of the unknowns. Specifically, the last  $m - (k + 2)$  elements in each column  $k$  are set to arbitrary values, i.e.  $s_{ik} = w_{ik}$  for  $i = k + 3, \dots, m$  and for  $k = 1, \dots, n$ . In the code supplied they set  $w_{i1} = 0$  for  $i = 4, \dots, m$ , and for  $k = 2, \dots, n$  they draw  $w_{ik}$  randomly from a uniform distribution on  $[0, 1]$ . This is possible because the exact Kollo skewness structure is derived entirely from the first few elements in each column of  $\mathbf{S}_{mn}$ . The vast majority of elements in each simulation have no effect on the value of Kollo skewness.

Given a set of arbitrary values, the HPSW algorithm attempts to solve (17-1) to (17-4). However, it is not always possible to find a solution. Also, the additional restriction that each simulation has exact Kollo skewness drastically complicates the computation. As a result, the HPSW algorithm is much slower than the original ROM simulation algorithm of Ledermann et al. (2011). On closer inspection the algorithm can be made much faster if we can minimize the number of trials taken to produce a set of arbitrary values for which (17-1) to (17-4) actually has real solutions.

The aim of our work is to extend and modify the HSPW algorithm to improve the way that arbitrary values are selected. We introduce the term admissible to refer to arbitrary values  $w_{ik}$  for which the system (17-1) to (17-4) has real solutions, that is, the code for the HPSW algorithm works. This motivates our development in Section 3.1 of necessary and sufficient conditions for arbitrary values to be admissible. Section 4 demonstrates how these conditions are used to substantially decrease the failure rate of the HPSW algorithm and thereby decrease the time taken for simulations.

Even when speed is not an issue, Section 3.2 explains how to modify the way that arbitrary values are selected to improve the distributional features of the simulations. Typically, neither zero nor random uniform arbitrary values will be appropriate – except perhaps for some special wave dynamic applications briefly referred to above. We show how to bootstrap admissible arbitrary values (if observations on the random variables are available) and how to draw them from parametric distributions that may reflect the desired properties of the marginal densities far better than simply employing a random uniform distribution.

### 3 Theoretical Results

Referring to their exact Kollo skewness algorithm, Hanke et al. (2017) state: “In this procedure, arbitrary values can be prescribed on several occasions. By varying these values, e.g. by setting them as random values, different  $L$  matrices can be constructed, all of which exactly match the pre-specified Kollo skewness vector.” However, we find that equations (17-1) to (17-4) cannot always be solved this way. For example, rewriting equation (17-2) as

$$s_{1k}^2 + \dots + s_{k+2,k}^2 = m - \sum_{i=k+3}^m w_{ik}^2.$$

which clearly has no real root when the random arbitrary values  $w_{ij}$  are such that  $\sum_{i=j+3}^m w_{ij}^2 > m$ . Therefore, in Section 3.1 we establish the necessary and sufficient conditions for the arbitrary values to be admissible, i.e., all the equations in the HPSW algorithm can be solved in the real numbers.

Then we discuss efficient methods for selecting admissible arbitrary values. In the code provided by HPSW the arbitrary values for the first column are set to zero, i.e.  $w_{i1} = 0$  for  $i \geq 3$  and the values in the other columns are randomly drawn, independently from a uniform distribution. However, in this case the target statistics, i.e. the mean, covariance matrix and Kollo skewness are derived from just a few non-arbitrary values. Another undesirable consequence is that each simulation has excessively high kurtosis. In Section 4.2 we use a numerical analysis to investigate these problematic features in more detail.

In this section we present necessary and sufficient conditions for arbitrary values to be admissible so that the code for HPSW will not fail. Then Section 3.2 proposes two new ways to generate arbitrary values, i.e. using a statistical bootstrap and a parametric distribution, which are more appropriate and yield a much higher success rate. Finally we prove a result that allows one to use *sample concatenation*, i.e. to join several small sub-samples into one simulation. In Section 3.3 we provide sufficient conditions for Kollo skewness to remain unchanged under concatenation.

#### 3.1 Necessary and Sufficient Conditions

Following 2.2 we suppose that the last  $m - (k + 2)$  elements in each column  $k$  are set to arbitrary values. Now we establish necessary and sufficient conditions for these arbitrary values to be admissible. The equations (17-1) to (17-4) of the HPSW algorithm should be solved iteratively, for  $j = 1, 2, \dots, n$ . First consider the case  $j = 1$ . Setting  $s_{ij} = w_{ij}$  for  $i = 4, \dots, m$  we can simplify and

rewrite the system (17-1) to (17-4) as the following three equations:

$$s_{11} + s_{21} + s_{31} = - \sum_{i=4}^m w_{i1} =: a \quad (18-1)$$

$$s_{11}^2 + s_{21}^2 + s_{31}^2 = m - \sum_{i=4}^m w_{i1}^2 =: b \quad (18-2)$$

$$s_{11}^3 + s_{21}^3 + s_{31}^3 = mp_1 - \sum_{i=4}^m w_{i1}^3 =: c. \quad (18-3)$$

**Lemma 1.** *A necessary and sufficient condition for the system (18-1) to (18-3) to have real solutions for  $s_{11}, s_{21}$  and  $s_{31}$  is:*

$$\left(b - \frac{a^2}{3}\right)^3 \geq 6 \left(c - ab + \frac{9}{2}a^3\right)^2. \quad (19)$$

The proof is in Appendix A. Now consider the case when  $j = 2, \dots, n$ . The system (17-1) to (17-4) are solved iteratively. So we assume that the system (17-1) to (17-4) is solvable in the real numbers for  $j = 1, \dots, k-1$ , and then seek necessary and sufficient conditions for the system to be solvable when  $j = k$ . In this case, the system (17-1) to (17-4) is most succinctly expressed in matrix form, as:

$$\mathbf{U}\mathbf{y} = \mathbf{v}, \quad (20)$$

$$\mathbf{y}'\mathbf{y} = m - \sum_{i=k+3}^m w_{ik}^2. \quad (21)$$

where  $\mathbf{y}$  is a column vector containing all the variables we want to solve, i.e.  $(s_{1,k}, \dots, s_{k+2,k})'$  and

$$\mathbf{U} = \begin{bmatrix} s_{11}^2 & s_{21}^2 & \cdots & s_{k+2,1}^2 \\ s_{11} & s_{21} & \cdots & s_{k+2,1} \\ s_{12} & s_{22} & \cdots & s_{k+2,2} \\ \vdots & \vdots & \vdots & \vdots \\ s_{1,k-1} & s_{2,k-1} & \cdots & s_{k+2,k-1} \\ 1 & 1 & 1 & 1 \end{bmatrix}, \mathbf{v} = \begin{bmatrix} mp_k - \sum_{i=k+3}^m s_{i1}^2 w_{ik} \\ - \sum_{i=k+3}^m s_{i1} w_{ik} \\ - \sum_{i=k+3}^m s_{i2} w_{ik} \\ \cdots \\ - \sum_{i=k+3}^m s_{i,k-1} w_{ik} \\ - \sum_{i=k+3}^m w_{ik} \end{bmatrix}.$$

Thus  $\mathbf{U}$  is a  $(k+1) \times (k+2)$  coefficient matrix and  $\mathbf{v}$  is a column vector. In practical applications we have always found that the column span of  $\mathbf{U}$  equals  $k+1$ , i.e. the matrix is full row rank. However, in some applications it could be that they are not. So, let  $\mathbf{U}_1$  be a matrix containing all the linearly independent columns of  $\mathbf{U}$ , with the remaining columns in the matrix  $\mathbf{U}_2$ . Denote by  $\mathbf{U}_1^+$  the Moore-Penrose inverse of  $\mathbf{U}_1$  which is defined as  $\mathbf{U}_1^+ = (\mathbf{U}_1' \mathbf{U}_1)^{-1} \mathbf{U}_1'$ .

**Theorem 1.** *Admissible arbitrary values exist for the HPSW algorithm if and only if the following three conditions are satisfied:*

(i) Lemma 1 holds for the first column of  $\mathbf{S}_{mn}$  - i.e. the arbitrary values selected in the first column of  $\mathbf{S}_{mn}$  satisfy (18-1) - (18-3) and (19); and

(ii) Assuming that the admissible arbitrary values exist for the 1 to  $k - 1$  columns, the arbitrary values selected in the  $k$ -th column ( $k = 2, \dots, n$ ) of  $\mathbf{S}_{mn}$  should have

$$\text{Rank}(\mathbf{U}) = \text{Rank}([\mathbf{U}, \mathbf{v}])$$

where  $[\mathbf{U}, \mathbf{v}]$  is the augmented matrix; and

(iii) Assuming that the admissible arbitrary values exist for the 1 to  $k - 1$  columns, the arbitrary values selected in the  $k$ -th column ( $k = 2, \dots, n$ ) of  $\mathbf{S}_{mn}$  should satisfy

$$\mathbf{g}' \mathbf{G}^{-1} \mathbf{g} - \mathbf{v}' (\mathbf{U}_1 \mathbf{U}_1')^+ \mathbf{v} \geq \sum_{j=i+3}^m w_{j_i}^2 - m$$

where

$$\mathbf{G} = \mathbf{I} + \mathbf{U}_2' (\mathbf{U}_1 \mathbf{U}_1')^+ \mathbf{U}_2 \quad \text{and} \quad \mathbf{g} = \mathbf{U}_2' (\mathbf{U}_1 \mathbf{U}_1')^+ \mathbf{v}.$$

This result allows a modification of HPSW which substantially improves the efficiency of the algorithm because the time spent on checking these conditions is much less than running an optimization algorithm to search for real roots of a very large number of equations. In particular, we avoid the unnecessary time spent on searching for solutions when the arbitrary values are inadmissible.

The following criteria for zero arbitrary values to be admissible is also proved in Appendix A:

**Corollary 1.** Zero arbitrary values  $w_{ik} = 0$  are admissible if and only if

$$p_1^2 \leq \frac{m}{6} \quad \text{and} \quad p_k^2 \leq \frac{t}{m} + \frac{m}{(k+1)(k+1)} \quad \forall k > 1,$$

where  $t = s_{11}^4 + s_{21}^4 + s_{31}^4 - m \left( \frac{m}{k+1} + p_1^2 + \dots + p_{k-1}^2 \right) > 0$

These conditions show that the HPSW algorithm is more likely to fail with zero arbitrary values when an element  $p_k$  of the rotated Kollo skewness is large and the sample size  $m$  is small.

### 3.2 Novel Methods for Generating Non-Zero Admissible Arbitrary Values

The conditions of Corollary 1 may not always hold but they are still less strict than the conditions of Theorem 1 with non-zero arbitrary values. However, we do not advise this practice, because then all the structure (i.e. the mean, covariance matrix and Kollo skewness) is derived from the first  $k + 2$  elements in the  $k$ -th column, for  $k = 1, \dots, n$ . This can cause unwanted distortions in the simulations, such as excessively high kurtosis and many extreme values. Clearly, we need to choose arbitrary values more carefully so here we propose two novel approaches for generating non-zero admissible arbitrary values.

Suppose the target moments are derived from a sample  $\mathbf{X}_{ln}^*$  where  $l$  is the number of observations and  $n$  is the number of variables – we distinguish this from  $\mathbf{X}_{mn}$  i.e. the samples generated using ROM simulation. We derive the corresponding scaled  $L$  matrix using a rotation matrix  $\mathbf{\Omega}_n$  as:

$$\mathbf{S}_{ln}^* = \left( \mathbf{X}_{ln}^* - \mathbf{1}_l \boldsymbol{\mu}'_n \right) \mathbf{A}_n^{-1} \mathbf{\Omega}_n. \quad (22)$$

For each column  $k$  we bootstrap  $m - (k + 2)$  arbitrary values from the corresponding column of  $\mathbf{S}_{ln}^*$  and we denote these bootstrapped values  $z_{ik}$ ,  $i = k + 3, \dots, m$ . Note that the HPSW algorithm does not impose any restriction on the dependency between columns of arbitrary values. In this paper we simply do this bootstrap independently, column by column, a simplistic approach which seems desirable anyway because the columns of  $\mathbf{S}_{mn}$  should have zero correlation. Based on these arbitrary values, the next task is to solve equations (17-1) to (17-4) to obtain columns with exactly zero mean, unit standard deviation and zero pair-wise correlation – as well as exact Kollo skewness.

For each bootstrapped sample we need to verify a solution to the simultaneous equations (17-1) to (17-4). Now, since each column of  $\mathbf{S}_{ln}^*$  has zero mean and unit standard deviation, it may well be that  $\sum_{i=k+3}^m z_{ik}^2 \geq m$  and in this case equation (17-2) has no real roots. Therefore, we set

$$\bar{z} = \frac{1}{m - (k + 2)} \sum_{i=k+3}^m z_{ik} \quad \text{and} \quad s_z^2 = \frac{1}{m - (k + 2)} \sum_{i=k+3}^m (z_{ik} - \bar{z})^2,$$

and transform the bootstrapped values  $z_{ik}$  to  $w_{ik}$  given by:

$$w_{ik} = \sigma \left( \frac{z_{ik} - \bar{z}}{s_z} \right), \quad i = k + 3, \dots, m. \quad (23)$$

Now,  $\sigma \in (0, 1)$  is set by the user to ensure that  $\sum_{i=k+3}^m z_{ik}^2 < m$ . Lower values of  $\sigma$  are more likely to result in real roots for (17-2) although no positive target value of  $\sigma$  is guaranteed to work. There is a trade off between setting a high  $\sigma$  to maximize sampling variation in the bootstrap and a low  $\sigma$  which reduces the failure rate. We still need to solve the whole system (17-1) to (17-4) and by virtue of simulation there will always be some values for which there is no solution. See Section 4.1 for an analysis of various judicious values for  $\sigma$  in an empirical application of failure rates.

As an alternative to bootstrapping we may select the arbitrary values from some assumed distributions, such as may be required in financial applications like risk management and portfolio optimization. This way, we combine univariate MC simulation with solving equations (17-1) to (17-4). As with the bootstrap, we may draw columns of arbitrary values independently from any set of univariate marginal distributions which – if we wish to exploit the maximum distributional flexibility of ROM simulation – can be chosen to have very different statistical properties. Nevertheless, when we do an empirical comparison of failure rates in Section 4.1 we shall only consider arbitrary values that are drawn from the same distribution family for each marginal, including the normal, skew-normal, beta and normal inverse Gaussian. In Appendix B we derive some additional theoretical results on failure rates but only for the normal distribution, showing that the  $\sigma$  resulting in admissible arbitrary values increases monotonically with any given failure rate  $\alpha$ , with  $\sigma$  and

$\alpha$  ranging between 0 and 1. The proof, which is essentially based on the central limit theorem, is lengthy and tedious. To prevent the paper becoming too overwhelming, we do not discuss this result further in the main text, but refer readers to Appendix B.

### 3.3 Sample Concatenation

Sample concatenation refers to the idea of “stitching” a finite number of samples to form a larger sample. In mathematical notation, let  $\mathbf{M}^{(k)}$ ,  $k = 1, 2, \dots, N$  be  $N$  sample matrices, each with dimension  $m_k \times n$ , then the sample concatenation of  $\mathbf{M}^{(k)}$  leads to a larger sample  $[\mathbf{M}^{(1)'}, \dots, \mathbf{M}^{(N)'}]'$ . Ledermann et al. (2011) first apply the sample concatenation method in ROM simulation. They show that the mean and covariance matrix of the concatenated samples are preserved if each constituent has identical mean and covariance matrix. The following theorem shows that Kollo skewness is also preserved under sample concatenation.

**Theorem 2.** *Let  $\mathbf{M}^{(k)}$  be a scaled  $L$  matrix of dimension  $m_k \times n$  with  $m_k \geq n + 2$ . Denote the  $i^{\text{th}}$  row of  $\mathbf{M}^{(k)}$  by  $\mathbf{r}_i^{(k)}$ , for  $i = 1, \dots, N$  where  $N$  is the number of concatenations. Then the Kollo skewness of the concatenated sample is the weighted sum of their Kollo skewnesses, i.e.*

$$\begin{aligned} \tau \left( \begin{bmatrix} \mathbf{M}^{(1)} \\ \vdots \\ \mathbf{M}^{(N)} \end{bmatrix} \right) &= \frac{1}{m_1 + \dots + m_N} \left( \sum_{i=1}^{m_1} (\mathbf{r}_i^{(1)} \mathbf{1}_n)^2 \mathbf{r}_i^{(1)'} + \dots + \sum_{i=1}^{m_N} (\mathbf{r}_i^{(N)} \mathbf{1}_n)^2 \mathbf{r}_i^{(N)'} \right) \\ &= \frac{1}{m_1 + \dots + m_N} \left( m_1 \tau \left( \mathbf{M}^{(1)} \right) + \dots + m_N \tau \left( \mathbf{M}^{(N)} \right) \right), \end{aligned} \quad (24)$$

It follows from Theorem 2 that Kollo skewness is invariant under sample concatenation, provided it is achieved via a set of (scaled)  $L$  matrices having identical dimensions and the same Kollo skewness.

In practice, we can utilise the sample concatenation method to improve the statistical features in the ROM simulations. For instance, consider the extreme case where all arbitrary values for  $n$  variables are zero so that a direct application of the HPSW algorithm yields only  $n + 2$  rows with non-zeros values. This results in some strange features especially when the simulation size  $M$  is large. By contrast, concatenation allows us to split  $M$  into  $N$  blocks, and apply the HPSW algorithm separately for each block. This way we have far fewer zero entries. The number of zero rows reduces from  $M - (n + 2)$  to  $M - N(n + 2)$  while leaving the sample mean, covariance and Kollo skewness invariant. In addition, the concatenated ROM simulations have much lower marginal kurtosis. We shall illustrate the use of concatenation in practice in Section 4.2 and see the algorithm in Appendix C.

## 4 Empirical Results

Here we present three applications of ROM simulation with exact Kollo skewness. The first applies our modification of HPSW to simulate the unconditional (rather than dynamic) properties of financial data by targetting multivariate moments derived from some real historical data. Here we

focus on the quantities that are most pertinent to our theoretical results, i.e. the rotated Kollo skewness vector. Section 4.1 presents results on the failure rate of our modified HPSW algorithm based on drawing arbitrary values from different distributions, finding that lowest failure rates are observed when bootstrapping from a sample. We also examine the sampling error when the standard bootstrap is applied to generate simulations from a sample, thus illustrating the advantage of ROM simulation with exact Kollo skewness. Section 4.2 presents a detailed evaluation of failure rates for the HPSW algorithm when all arbitrary values are drawn from a  $\mathcal{N}(0, \sigma^2)$  distribution. This way, we derive empirical guidelines on the upper limit of  $\sigma$  for the HPSW algorithm to work, i.e. for the arbitrary values to be admissible. The final empirical study in Section 4.3 depicts the extreme kurtosis that is implicit in a standard application of HPSW, with admissible arbitrary values drawn from  $\mathcal{N}(0, \sigma^2)$ . Then we illustrate how the application of concatenation reduces this kurtosis considerably.

#### 4.1 Application to Real Data

Two sets of multivariate data are depicted in Figure 1. On the left are returns on three cryptocurrencies. The data are hourly historical returns on US dollars prices for Bitcoin (BTC), Ether (ETH), and Litecoin (LTC) from 1 January 2017 to 14 August 2020 – so there are over 27,000 data points in each series. The other data set is for eleven S&P 500 industry sector indices consisting of companies in the same or related industries. Here we employ daily returns from 16 October 2001 to 18 September 2020 and there are over 4,500 data points in each series. The right panel of Figure 1 only depicts three of the eleven indices, viz. Energy, Finance and Real Estate.

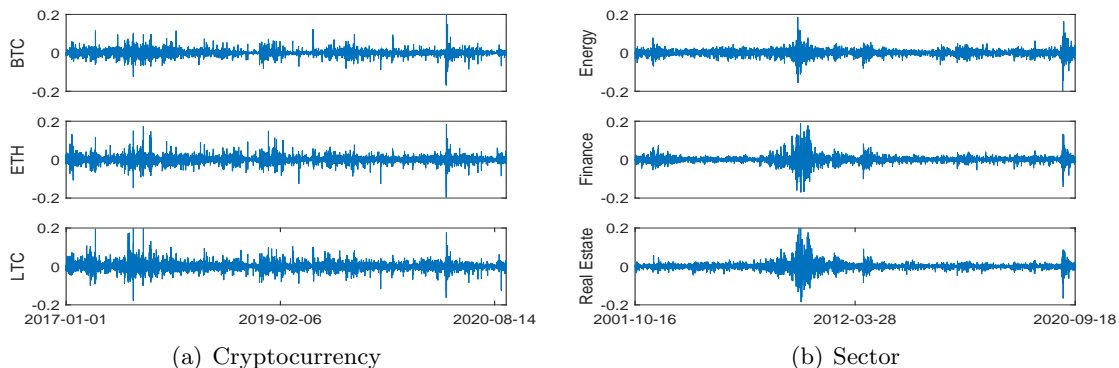


Figure 1: **Time series of financial returns.**

Panel (a) exhibits the hourly returns on three cryptocurrencies: BTC, ETH and LTC and panel (b) exhibits the daily returns for three S&P 500 sector indices, viz. Energy, Finance and Real Estate

First we derive the Kollo skewness vector using a rolling window to illustrate the range of values that could be expected using real data. For the hourly cryptocurrency data, setting the length of rolling window 720 points (i.e. around one month) all elements in the Kollo skewness vector lie in the range  $[-10, 10]$  with most sampling variability in  $\tau_1$ , as shown in panel (a) of Figure 2. In particular, the cryptocurrency market-wide price crash on 12 January 2020 (Black Thursday) is evident from the dip in Kollo skewness down to almost  $-10$ . On the right, panel (b) of Figure 2

depicts the rotated Kollo skewness using the matrix  $\Omega_n$  specified in Appendix C. Here we note that  $p_1, p_2$  and  $p_3$  lie in the range  $[-3, 3]$ .

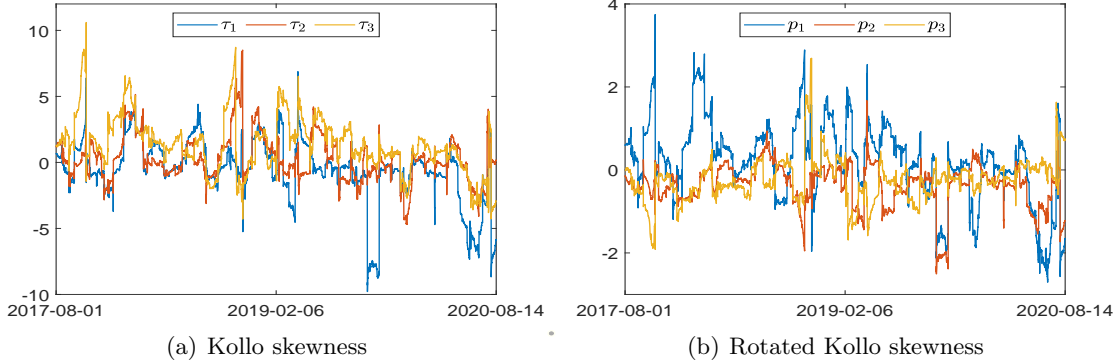


Figure 2: **Kollo skewness  $\tau_3 = [\tau_1, \tau_2, \tau_3]$  and rotated Kollo skewness  $p_3 = [p_1, p_2, p_3]$  for the cryptocurrency hourly returns.**

Panel (a) is the Kollo skewness and panel (b) is the rotated Kollo skewness. The Kollo skewness and its rotation are computed on a rolling window of 720 hourly returns.

Figure 3 illustrates the results of similar computations for the S&P 500 sector data, this time using a one-year rolling window containing 250 points. To keep consistency with Figure 1 we only depict  $\tau_1, \tau_7$  and  $\tau_{11}$ , i.e. the Energy, Finance and Real Estate sector results, but the 11-dimensional Kollo skewness and its rotated value are in a similar range for the other sectors. The Kollo skewness takes a very similar range to the cryptocurrency data except during the sector-wide crash in the S&P 500 index in March 2020. For example the low values of  $\tau_1$  during the first half of 2018 were caused by an upward surge in oil prices. Similarly, the upward spike in  $\tau_7$  on 16 March 2020 resulted from an extreme return in the Finance sector index, of around  $-14\%$ . Apart from these extreme values, we note that most elements in the rotated Kollo skewness lie in the range  $[-1, 1]$ .

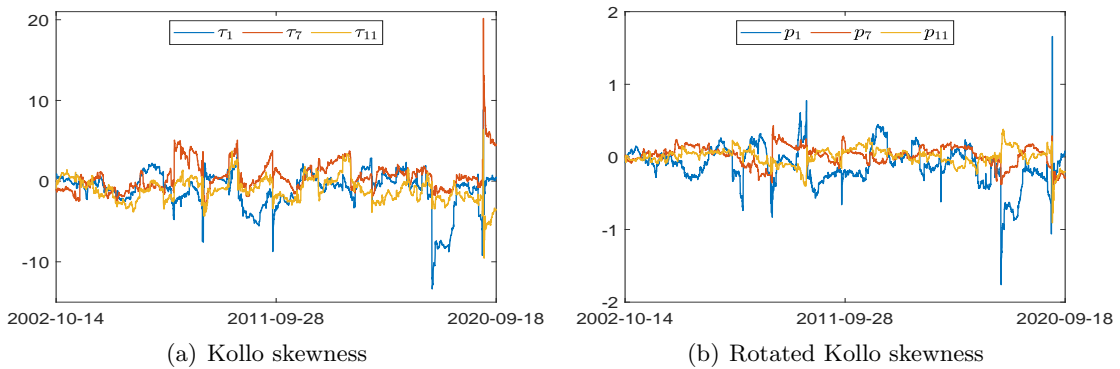


Figure 3: **The Energy, Finance and Real Estate elements of Kollo skewness  $\tau_{11}$  and its rotation based the daily returns on S&P 500 sector indices.**

Panel (a) is the Kollo skewness and panel (b) is the rotated Kollo skewness. The Kollo skewness and its rotation are computed on a rolling window 250 daily returns.

Next we apply the modified HPSW algorithm to simulate the three-dimensional cryptocurrency hourly returns, based on some historical values for mean, covariance and Kollo skewness, i.e. certain

empirical quantiles derived from the sample exhibited in Figure 2. We design the experiment with extreme values and a median value by selecting target samples with corresponding 1%, 50% and 99% quantiles of  $p_1$ . To examine the failure rate of the algorithm for different arbitrary values we focus on the first element of  $\mathbf{p}_n$  because the most strict conditions are the cubic restriction on the first column of  $\mathbf{S}_{mn}$ , i.e. equation (17-1). That is, the  $p_1$  time series exhibited in Figure 2 panel (b) is used to generate a histogram and the  $q$ -quantile is identified from this, for  $q = 1\%, 50\%$  and  $99\%$ . For each quantile of  $p_1$ , the corresponding values for  $p_2$  and  $p_3$  are those observed for the same time period, based on same 720 observations for each variable. These  $\mathbf{p}_3$  vectors are named Case 1, Case 2, and Case 3 in the left-hand column of Table 1. The arbitrary values are selected using one of the methods described in Section 3.2. That is, we generate arbitrary values via bootstrapping and using several parametric distributions, viz. the Normal distribution (N), the Skew-Normal distribution (SN), the Beta distribution (Beta), and the Normal-Inverse Gaussian distribution (NIG). In each non-normal case we set  $\sigma = 1$  and fix the other parameters by fitting to each sample of 720 observations for each variable. This way, the arbitrary values are selected to reflect the properties of each marginal empirical distribution. Table 1 reports the failure rate, as a proportion of fails from a total 10,000 simulations, for different values of  $\tau_3$ ,  $m$  and  $\sigma$  as defined in (23). The parameters of each distribution are fixed throughout.

**Table 1: Failure rate of simulating real data**

The failure rate is the proportion of failed cases among 10,000 trails and reported as a percentage. A simulation fails if the arbitrary values in any column fail to meet necessary and sufficient conditions in Theorem 1. The simulations are for three target samples with different Kollo skewness and rotated Kollo skewness vectors (columns 2 and 3) and we simulate samples of size  $m = 500$  and  $m = 1000$  and compare the failure rate for different ways of generating arbitrary values: bootstrapping from historical data, assuming a normal distribution (Normal), a skewed-Normal distribution (SN), a Beta distribution (Beta), and a Normal-Inverse Gaussian distribution (NIG). For each approach, the failure rates are also computed for different values of  $\sigma$  in (23).

	$\tau_3$	$\mathbf{p}_3$	$\sigma^2$	Bootstrapping		Normal		SN		Beta		NIG	
				500	1000	500	1000	500	1000	500	1000	500	1000
1	$\begin{bmatrix} -6.44 \\ -2.22 \\ -2.97 \end{bmatrix}$	$\begin{bmatrix} -2.24 \\ -1.05 \\ 0.18 \end{bmatrix}$	0.7	35.62	7.56	100	97.93	96.83	0.01	0.08	0.18	36.79	4.97
			0.8	68.23	36.80	100	100	100	100	95.43	1.52	79.41	44.90
			0.9	83.67	75.13	100	100	100	100	99.98	99.91	90.63	84.63
2	$\begin{bmatrix} -1.09 \\ 1.25 \\ 1.08 \end{bmatrix}$	$\begin{bmatrix} 0.24 \\ -0.61 \\ 0.04 \end{bmatrix}$	0.7	34.99	31.97	0.01	0.02	1.85	0.53	0.94	0.27	38.77	34.60
			0.8	35.31	31.18	0.65	0.02	2.02	0.53	1.32	0.41	39.35	35.28
			0.9	46.84	46.67	100	97.86	76.44	71.77	79.28	73.18	57.59	54.07
3	$\begin{bmatrix} 2.47 \\ 3.82 \\ 5.90 \end{bmatrix}$	$\begin{bmatrix} 2.35 \\ -0.65 \\ -0.49 \end{bmatrix}$	0.7	44.52	9.44	100	100	99.72	0.03	0.14	0.39	37.85	4.75
			0.8	57.12	33.61	100	100	100	100	51.79	1.34	67.74	38.98
			0.9	74.57	69.05	100	100	100	100	99.51	99.32	87.65	82.21

As anticipated from our theoretical results, the smallest failure rates occur for larger  $m$  and smaller  $\sigma^2$ . In addition, we find that extremely skewed data (Case 1 and Case 3) yields a substantially higher failure rate than moderately skewed data (Case 2). Of all methods for generating arbitrary values the historical bootstrap has the most stable performance and much the lowest failure rate except when  $m$  is large and  $\sigma^2$  is small. Comparing the failure rate for the parametric distributions we find the normal distribution only works well around the median range, i.e. when the rotated Kollo skewness is about  $\mathbf{0}$ . This is easy to understand, because multivariate independent

normal distributions always have zero Kollo skewness, so the HPSW algorithm will often fail when simulating extremely skewed data.

Notice that Table 1 suggests that bootstrapping from a historical sample (when possible) produces the lowest failure rates in general. This is not surprising, and in fact, in some sense tautological: the arbitrary values generated using the historical data should retain the most of the properties from the historical data. We emphasize that our bootstrap ROM method is fundamentally different from the standard bootstrap approach: our methods are capable of generating exactly zero sampling error in each and every ROM simulation, but a standard bootstrap approach would inevitably suffer from sampling errors. To illustrate the advantage of the proposed ROM approach, next we examine the numerical sampling errors for the Kollo skewness vector of the standard bootstrap approach.

**Table 2: Root mean square sampling errors of multivariate moments in statistical bootstrapping.**

The first three columns illustrate the first three moments for three sets of samples each of size 720 and the fourth column states the size of each bootstrap. The mean and standard error (in parentheses, below) derived using (25) are in columns 5–7, computed using 10,000 bootstraps for each. The last three columns are the ratio of the average RMSE to its standard error and we use \*, \*\* or \*\*\* to denote significantly greater than 0 at the 90%, 95% or 99% confidence level, respectively.

$\boldsymbol{\mu}_3$ ( $10^{-5}$ )	$\mathbf{V}_3$ ( $10^{-5}$ )			$\boldsymbol{\tau}_3$	$m$	RMSE			Ratio		
						$\boldsymbol{\mu}_3$ ( $10^{-5}$ )	$\mathbf{V}_3$ ( $10^{-5}$ )	$\boldsymbol{\tau}_3$	$\boldsymbol{\mu}_3$	$\mathbf{V}_3$	$\boldsymbol{\tau}_3$
$\begin{bmatrix} 6.91 \\ 20.53 \\ 0.06 \end{bmatrix}$	$\begin{bmatrix} 2.93 & 2.99 & 2.74 \\ 2.99 & 4.40 & 3.49 \\ 2.74 & 3.49 & 3.65 \end{bmatrix}$			$\begin{bmatrix} -6.44 \\ -2.22 \\ -2.97 \end{bmatrix}$	100	8.739 (5.827)	5.017 (3.855)	7.409 (3.131)	1.500*	1.302*	2.367***
					500	3.939 (2.449)	2.303 (1.624)	4.563 (2.875)	1.608*	1.418*	1.587*
					1000	2.823 (1.746)	1.607 (1.126)	3.141 (2.072)	1.617*	1.427*	1.516*
$\begin{bmatrix} -4.11 \\ 14.12 \\ -2.31 \end{bmatrix}$	$\begin{bmatrix} 2.61 & 2.59 & 2.52 \\ 2.59 & 4.74 & 3.96 \\ 2.52 & 3.96 & 5.51 \end{bmatrix}$			$\begin{bmatrix} -1.09 \\ 1.25 \\ 1.08 \end{bmatrix}$	100	9.834 (5.817)	3.927 (2.989)	3.731 (1.735)	1.691**	1.314*	2.150**
					500	4.379 (2.506)	1.830 (1.193)	2.652 (1.188)	1.747**	1.534*	2.232**
					1000	3.111 (1.786)	1.301 (0.859)	1.892 (1.028)	1.742**	1.514*	1.841**
$\begin{bmatrix} -21.09 \\ 86.00 \\ -21.58 \end{bmatrix}$	$\begin{bmatrix} 26.56 & 25.41 & 27.88 \\ 25.41 & 43.41 & 32.83 \\ 27.88 & 32.83 & 41.75 \end{bmatrix}$			$\begin{bmatrix} 2.47 \\ 3.82 \\ 5.90 \end{bmatrix}$	100	28.530 (17.091)	28.750 (23.705)	7.314 (3.003)	1.669**	1.213	2.435***
					500	12.836 (7.634)	13.782 (9.385)	4.790 (2.365)	1.681**	1.469*	2.026**
					1000	9.114 (5.445)	9.768 (6.710)	3.270 (2.104)	1.674**	1.456*	1.554*

Table 2 reports sampling errors for the mean vector, covariance matrix and Kollo skewness vector when applying the statistical bootstrapping to the cryptocurrency historical returns. Again we set rotated Kollo skewness to Cases 1, 2 and 3 as described above for Table 1. Note that 720 hourly returns were used to generate each  $q$ -quantile. It is these returns that we use for each case of the statistical bootstrap. This way, we know the multivariate sample moments and we use 720 data points to bootstrap samples of a fixed size  $m$ , with replacement. In order to preserve correlation, we randomly select entire rows of the target sample. We define the root mean square error (RMSE) to be the square root of the total squared difference between the target moment and the sampled moment. That is, for general  $n$ , if  $\mu_i, V_{ij}, \tau_i$  are the elements of the target mean  $\boldsymbol{\mu}_n$ , covariance  $\mathbf{V}_n$  and Kollo skewness  $\boldsymbol{\tau}_n$  respectively and  $\hat{\mu}_i, \hat{V}_{ij}, \hat{\tau}_i$  are the corresponding elements of the sample moments obtained by bootstrapping, the RMSE for these moments are defined, respectively, by:

$$\sqrt{\sum_i^n (\mu_i - \hat{\mu}_i)^2}, \sqrt{\sum_{i,j}^n (V_{ij} - \hat{V}_{ij})^2}, \sqrt{\sum_i^n (\tau_i - \hat{\tau}_i)^2}. \quad (25)$$

We do 10,000 bootstraps so the RMSE above are calculated 10,000 times, and this way we obtain both a mean and a standard error of each quantity in (25). Table 2 reports the results, for samples of sizes  $m = 100, 500$  and  $1000$ . The right-hand panel reports the ratio of the mean to the standard error, using the central limit theorem to derive critical values for significance. From this it is clear that sampling error is significant for both the mean and Kollo skewness, especially when  $m$  is small.

## 4.2 Numerical Results on Failure Rates

The necessary and sufficient conditions derived in Theorem 1 depend on the system dimension  $n$ , the simulation sample size  $m$  and the target rotated Kollo skewness  $\mathbf{p}_n$ . How does the failure rate of our modified HPSW algorithm change with different  $n$ ,  $m$ , and  $\mathbf{p}_n$ ? To answer this, Table 3 reports the failure rate in 10,000 simulations for different sets of  $(n, m, \mathbf{p}_n)$ . In addition to the overall failure rate for all variables in the system, we also report the proportion of failures in only the first column of  $\mathbf{S}_{mn}$ . This is because the conditions of Lemma 1 for the first column have an additional cubic equation which is the most difficult one to solve. For simplicity, Table 3 only reports results for arbitrary values based on  $\mathcal{N}(0, \sigma^2)$  with the same  $\sigma$  for each column of  $\mathbf{S}_{mn}$ . Since our real data have rotated Kollo skewness with all elements most commonly within the range  $[-1, 1]$ , as previously remarked in Section 4.1 we consider two special cases: when  $\mathbf{p}_n = \mathbf{0}_n$  so the multivariate data is not skewed at all, and  $\mathbf{p}_n = \mathbf{1}_n$  so the data are skewed but not too extremely. To examine the effect of the system dimension, we set  $n = 5$  and  $n = 20$ .

Table 3: **The failure rate for all-zeros and all ones  $\mathbf{p}_n$  with  $n = 5$  and  $n = 20$ .**

The arbitrary values are independently drawn 10,000 times for each column from  $\mathcal{N}(0, \sigma^2)$ . If they are inadmissible for any column we record a failed simulation. We denote the failure rate for the first column alone by  $\alpha_1$ . The overall failure rate  $\alpha$  is the proportion of total failed simulations. We report numerical failure rates for  $n = 5$  and  $n = 20$ , and set the rotated Kollo skewness  $\mathbf{p}_n = \mathbf{0}_n$  and  $\mathbf{p}_n = \mathbf{1}_n$  for different  $n$ . In each case, we compute the failure rate (in percent) for different simulation sample sizes, i.e. with  $m = 50, 100, 500, 1000$  and with  $\sigma^2$  varying from 0.6 to 0.9.

$n$	$\mathbf{p}_n$	$\sigma^2$	$m = 50$		$m = 100$		$m = 500$		$m = 1000$	
			$\alpha_1$	$\alpha$	$\alpha_1$	$\alpha$	$\alpha_1$	$\alpha$	$\alpha_1$	$\alpha$
5	$\mathbf{0}_5$	0.6	0	0.62	0	0.40	0	0.17	0	0.23
		0.7	0.31	12.34	0	1.74	0	0.18	0	0.29
		0.8	10.83	70.80	1.25	38.67	0	0.51	0	0.16
		0.9	49.83	99.50	34.65	98.69	0.10	53.51	0	14.68
20	$\mathbf{0}_{20}$	0.6	0.01	63.56	0	28.06	0	0.63	0	0.18
		0.7	0.44	99.78	0.01	99.36	0	1.74	0	0.15
		0.8	10.86	100	1.03	100	0	98.73	0	25.52
		0.9	49.49	100	34.50	100	0.06	100	0	100
5	$\mathbf{1}_5$	0.6	88.17	100	16.42	100	0	0.28	0	0.06
		0.7	98.75	100	97.10	100	0	48.29	0	0.39
		0.8	99.64	100	99.92	100	97.49	100	0.04	99.93
		0.9	99.76	100	100	100	100	100	100	100
20	$\mathbf{1}_{20}$	0.6	88.36	100	16.68	100	0	99.99	0	0.70
		0.7	98.68	100	96.98	100	0	100	0	100
		0.8	99.71	100	99.90	100	97.51	100	0.06	100
		0.9	99.81	100	100	100	100	100	100	100

For any given  $m$  and  $n$  in Table 3, the following properties are observed, all of which are expected from earlier discussions: the overall failure rates are always greater than the failure rates for the first column; when the target rotated Kollo skewness is  $\mathbf{p}_n = \mathbf{1}_n$  the failure rate is much higher than when  $\mathbf{p}_n = \mathbf{0}_n$ ; failure rates for the first column alone do not depend on  $n$ ; and as the dimension  $n$  increases so does the failure rate. We have also generated some interesting new results. First, the algorithm has a higher failure rate when  $m$  is small. For example, when  $\mathbf{p}_n = \mathbf{1}_n$  and  $m = 50$ , we find no set of admissible arbitrary values among all 10,000 trials – in both low and high dimensional systems. But when  $\mathbf{p}_n = \mathbf{1}_n$  and  $m = 1000$ , all trials succeed if we set  $\sigma^2 = 0.6$ . Secondly, for any given  $m$ ,  $n$  and  $\mathbf{p}_n$ , the failure rate in Table 3 is increasing with  $\sigma$ .

We conclude this subsection by exploring the failure rate for the first column of  $\mathbf{S}_{mn}$  because the cubic constraints in this case are the most exacting. If time is not an issue, a prolonged trial and error for arbitrary values may be acceptable. However, in some applications it can be important to perform a very large number of simulations in an extremely short time – for instance, when pricing financial products in an algorithmic trading strategy. In that case, we may wish to define a prescribed acceptable failure rate  $\alpha$ . e.g.  $\alpha = 0.05$ .

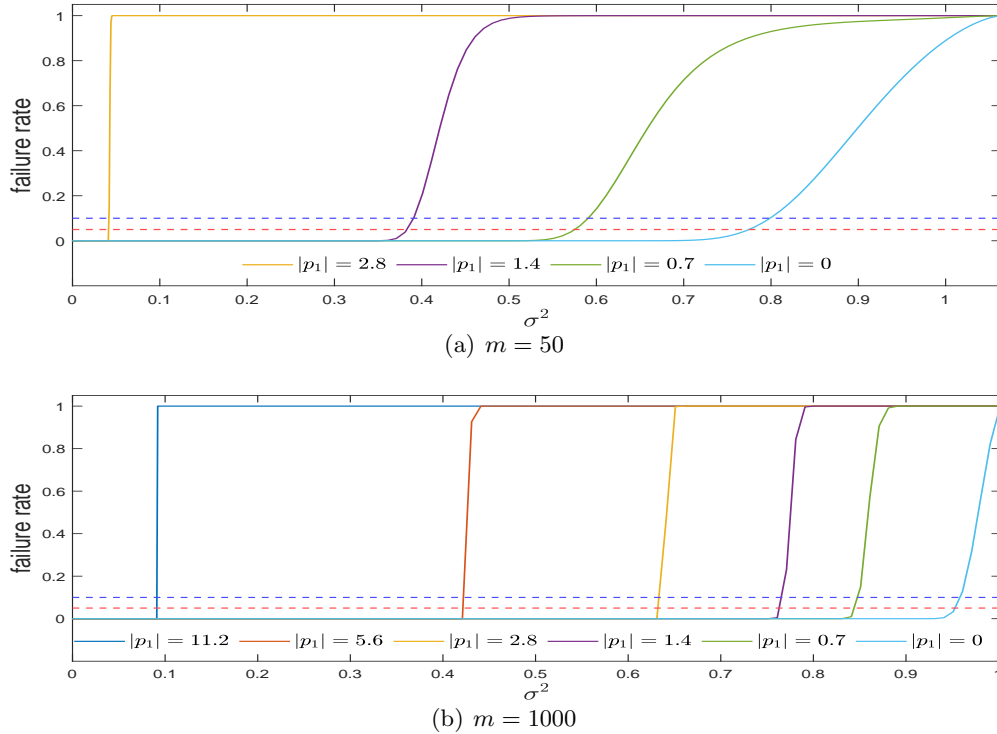


Figure 4: **The theoretical failure rate of the first column with different  $p_1$ .**

The upper plots (a) are for  $m = 50$  and those below (b) are for  $m = 1000$ . The arbitrary values in the first column are chosen from  $\mathcal{N}(0, \sigma^2)$ . The red and blue horizontal dashed line depict the failure rate at 5% and 10%.

For the case when arbitrary values are normal, Appendix B presents a theoretical result for the first column's failure rate – see equation (B.2). To illustrate this result, Figure 4 depicts theoretical failure rates when  $\sigma^2 \in \left[0, \frac{m}{m-3}\right]$ . for  $m = 50$  (above) and  $m = 1000$  (below) and for various value of rotated Kollo skewness between 0 and 11.2, as shown in the legend. All curves are monotonic increasing from 0 to 1 on the interval  $\sigma^2 \in \left[0, \frac{m}{m-3}\right]$  and there is an obvious jump in each curve

when either  $m$  or  $|p_1|$  are large. Comparing the cases  $m = 50$  and  $m = 1000$ , for any given failure rate  $\alpha$ , a larger sample size can allow for larger  $|p_1|$  with the same  $\sigma^2$ , or alternatively a greater  $\sigma^2$  for the same  $|p_1|$ . Therefore, when the target Kollo skewness is far away from  $\mathbf{0}_n$  we need to consider larger sizes of simulations and smaller  $\sigma^2$  to ensure a reasonably low failure rate.

These results provide a numerical answer to the question of how small  $\sigma$  should be to ensure admissibility. This is very useful to know, at least in those practical applications where retaining a maximum variability in arbitrary values is important. In this case, we should ensure that the algorithm’s failure rate is not so great that a ‘trial and error’ approach becomes extremely time consuming. Low values for  $\sigma$  are unlikely to produce realistic simulations except in some applications, and mentioned in the introduction.

When might a prescribed failure rate be useful? Much depends whether on the time taken for the algorithm to work, which itself depends on the dimension of the system. For instance, using the code that we provide with this paper running Python under Windows on a computer with Intel Core i5-8250U CPU, 3.41 GHz, and 8 GB RAM, it takes only 0.0375 seconds to generate 1000 simulations for a 20-dimensional system, but this is using zero arbitrary values when  $\boldsymbol{\tau}_n = \mathbf{0}_n$ . It takes 1.956 seconds to generate admissible arbitrary values for the same number of simulations from an auxiliary normal distribution  $\mathcal{N}(0, 0.5)$  and 4.706 seconds with the auxiliary distribution  $\mathcal{N}(0, 0.8)$ . These times increase rapidly with  $n$  especially when the target Kollo skewness is larger.

### 4.3 Kurtosis Reduction using Concatenation

Section 3 shows that setting arbitrary values to zero is less likely to result in failure of the HPSW algorithm than using the extensions that we propose. However, this practice results in some strange features which could be inappropriate for some simulation models. Consider an hypothetical example with  $n = 5$ ,  $m = 100$ , a target mean vector  $\mathbf{0}_5$ , a target covariance matrix  $\mathbf{1}_5$  and Kollo skewness vector  $\mathbf{1}_n$ . Figure 5 plots the resulting sequential graphs and histograms for the corresponding ROM simulations. As we know, all simulations contain almost all arbitrary values, which in this case are zeros, and only the first few elements are capturing the Kollo skewness structure. If required, an application of random permutation matrix in the ROM simulation can change the location of this activity, as discussed in Ledermann et al. (2011), but such patterns are not appropriate in many fields of application, as previously discussed.

In other applications, such as those in finance, the excessively high marginal kurtosis implicit in this type of application is unrealistic. In fact, because we always need to apply a variance reduction in equation (23) to ensure admissibility of the values selected, excessively high kurtosis may always a problem for some applications. To illustrate just how high the kurtosis can be, compare choosing arbitrary values from  $\mathcal{N}(0, 0.3)$  with those from  $\mathcal{N}(0, 0.6)$ , setting the same parameters as in Figure 5. The first column of Figure 6 exhibits the corresponding ROM simulations as both (a) sequential figures (above) and (b) histograms (below). The results for  $\sigma^2 = 0.3$  in blue show many extreme values and a much greater kurtosis than the result for  $\sigma^2 = 0.6$  in orange.

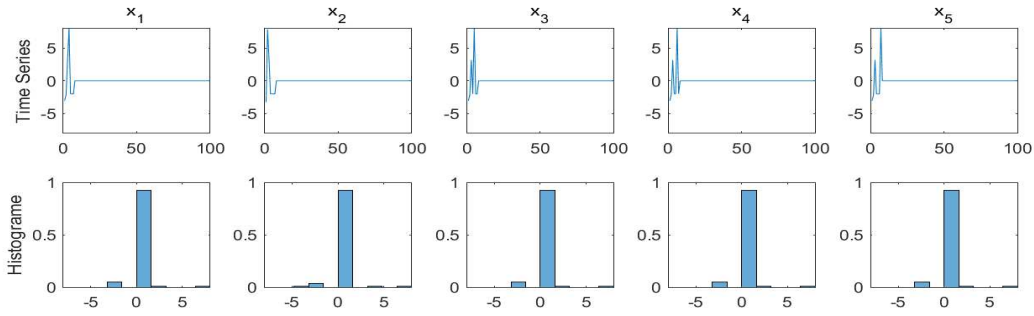
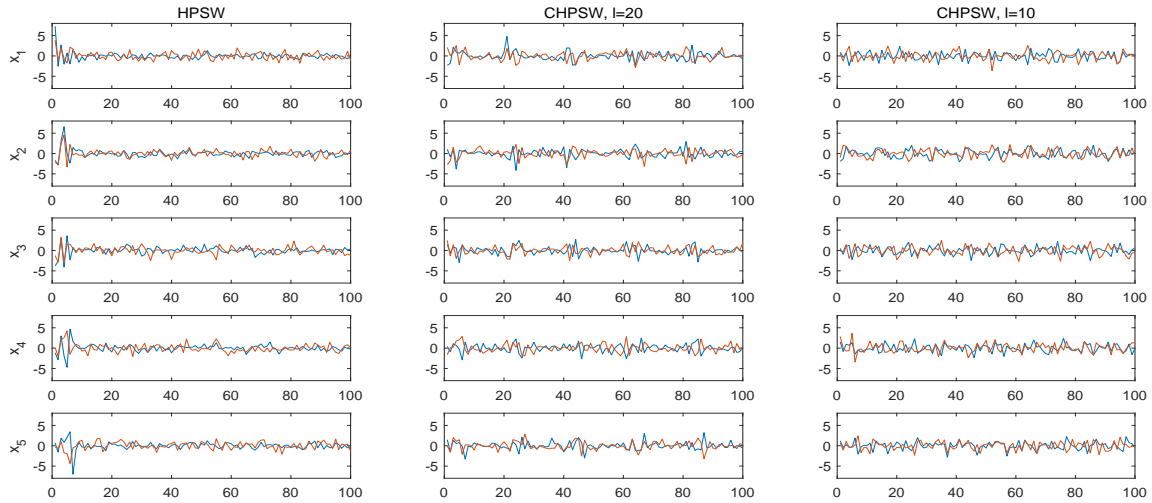
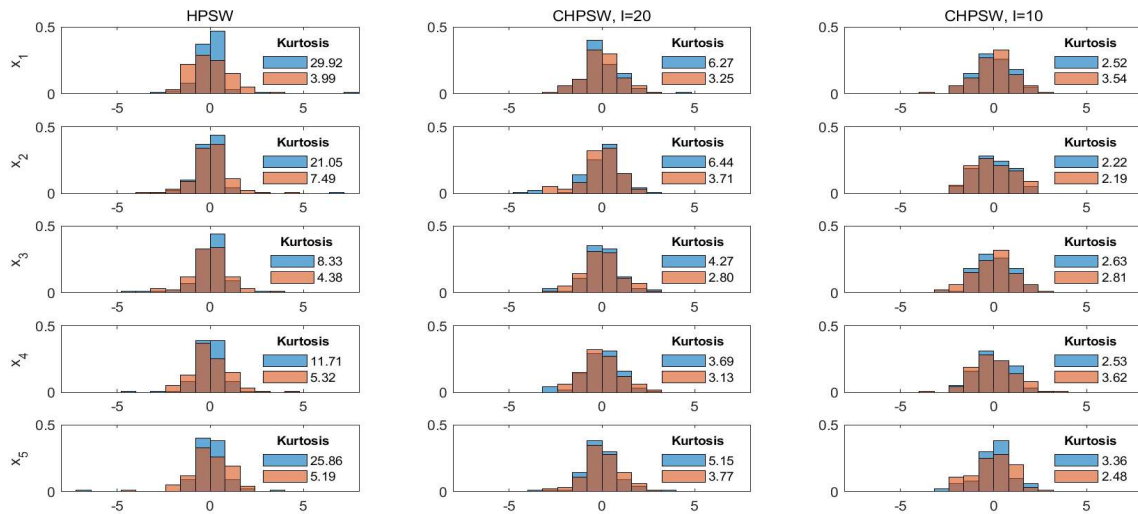


Figure 5: Samples generated by all-zero arbitrary values with  $m = 100$ ,  $n = 5$ ,  $\tau = 1_5$ . Here we depict  $x_1, \dots, x_5$  from left to right for sequential figures (above) and histograms (below).



(a)



(b) Kollo skewness

Figure 6: Sample generated by HPSW and CHPSW algorithms with  $n = 5$ ,  $m = 100$ ,  $\tau = 1_5$ . The left-hand column shows the results obtained using the HPSW algorithm. In the concatenation extension (CHPSW) the length of the sub-samples are  $l = 20$  (middle column) and  $l = 10$  (right-hand column). The rows correspond to variables  $x_1, \dots, x_5$ . The blue and orange shows the sample using admissible values from two normal distributions,  $\mathcal{N}(0, 0.3)$  (blue) and  $\mathcal{N}(0, 0.6)$  (orange).

To address this problem, Section 3.3 proposed another modification, the concatenated HPSW (CHPSW) algorithm, which is designed to preserve Kollo skewness while reducing marginal kurtosis. Figure 6 illustrates how this works in practice, by comparing our modified HPSW with the CHPSW algorithm based on two possible sub-sample sizes, i.e.  $l = 20$  (middle column) and  $l = 10$  (right-hand column). The results show how the moment structure is now spread out over the entire sample and the range of extreme values decreases as a result. This technique can be used to infer periodicity via the CHPSW algorithm which can be useful for simulating seasonal data. Otherwise, it can easily be eliminated by pre-multiplying with a random permutation matrix to re-order the observations. The histograms in Figure 6 also report the sample kurtosis. Without concatenation, marginal kurtosis is extremely high especially when arbitrary values are obtained using  $\mathcal{N}(0, 0.3)$  (blue). In each case and for each variable, concatenation reduces this, especially when the sub-sample size in the concatenation is small.

## 5 Summary and Conclusions

The HPSW simulation algorithm of Hanke et al. (2017) is an extension of ROM simulation that produces multivariate samples having exact Kollo skewness by solving a set of simultaneous non-linear equations which are generated from a very large number of so-called ‘arbitrary’ values. These values could be zero, or generated from some random variable  $W$ . We prove that some choices for  $W$  are inadmissible, in that it is never possible to find a set of arbitrary values for which the HPSW equations are solvable in the real numbers. That is, the trial-and-error approach to finding arbitrary values that is advocated by Hanke et al. (2017) may never work. Even if it does work, trying to solve the HPSW equations slows the algorithm down. To circumvent this problem we provide necessary and sufficient conditions on  $W$  to be admissible that are quick and easy to check.

Even if speed is not an issue, it is important to select admissible values that reflect the proper structure of the marginal densities. In the HPSW algorithm the Kollo skewness is matched using only the first few simulations on each variable and the code provided with Hanke et al. (2017) just sets all other simulations to zero, or it draws them randomly from a uniform distribution. However, this way, the marginal densities exhibit some highly idiosyncratic properties, including excessive kurtosis. We show that it is much better to draw the arbitrary values using a statistical bootstrap. Or, if no observations on the random variables are available, we develop a parametric approach which reduces the failure rate of HPSW while generating marginal densities without extreme kurtosis.

An empirical study shows how the failure rate depends on the choice of  $W$  and the simulation sample size. It is no surprise that drawing arbitrary values from a normal distribution (or any other symmetric distribution) will often fail when we target an extreme value for Kollo skewness, but even the skew-normal has 100% failure rate when the standard deviation is too high.

Although the failure rate increases with the variance of the arbitrary values, retaining variability in simulations is important for most practical applications. With this in mind we extend the HPSW algorithm by applying a novel result on the invariance of Kollo skewness under sample concatenation. Our empirical results show that this extension of the HPSW algorithm further enhances the features of marginal densities.

## References

- Adelfio, G., Chiodi, M., D'Alessandro, A., Luzio, D., D'Anna, G., and Mangano, G. (2012). Simultaneous seismic wave clustering and registration. *Computers & Geosciences*, 44:60–69.
- Alexander, C. and Ledermann, D. (2012). ROM simulation: Applications to stress testing and VaR. *Available at SSRN 2049239*.
- Avramidis, A. and Matzinger, H. (2002). Convergence of the stochastic mesh estimator for pricing American options. *Winter Simulation Conference Proceedings*, 2:1560–1567.
- Badano, A. and Samuelson, F. (2013). Uncertainty of Monte Carlo variance estimates: Application to the simulation of x-ray imaging detectors. *Progress in Biomedical Optics and Imaging - Proceedings of SPIE*, 8668.
- Bollerslev, T., Engle, R. F., and Nelson, D. B. (1994). Arch models. *Handbook of econometrics*, 4:2959–3038.
- Capriotti, L. (2008). Least-squares importance sampling for Monte Carlo security pricing. *Quantitative Finance*, 8(5):485–497.
- Cardano, G. (1968). *Ars Magna or the Rules of Algebra*. Dover Publications.
- Engle, R. F. (1982). Autoregressive conditional heteroscedasticity with estimates of the variance of United Kingdom inflation. *Econometrica: Journal of the Econometric Society*, pages 987–1007.
- Ferraz, V. and Moura, F. (2012). Small area estimation using skew normal models. *Computational Statistics and Data Analysis*, 56(10):2864–2874.
- Geyer, A., Hanke, M., and Weissensteiner, A. (2014). No-arbitrage ROM simulation. *Journal of Economic Dynamics and Control*, 45:66–79.
- Golub, G. H. and Van Loan, C. F. (2012). *Matrix Computations*, volume 3. JHU press.
- Gutjahr, S., Henze, N., and Folkers, M. (1999). Shortcomings of generalized affine invariant skewness measures. *Journal of Multivariate Analysis*, 71(1):1–23.
- Hanke, M., Penev, S., Schief, W., and Weissensteiner, A. (2017). Random orthogonal matrix simulation with exact means, covariances, and multivariate skewness. *European Journal of Operational Research*, 232(2):510–523.
- Hesterberg, T. (1996). Control variates and importance sampling for efficient bootstrap simulations. *Statistics and Computing*, 6(2):147–157.
- Hürlimann, W. (2013). Generalized Helmert–Ledermann orthogonal matrices and ROM simulation. *Linear Algebra and its Applications*, 439(7):1716–1729.
- Hürlimann, W. (2014). Market Value-at-Risk: ROM simulation, Cornish-Fisher VaR and Chebyshev-Markov VaR bound. *British Journal of Mathematics & Computer Science*, 4(13):1797.
- Hürlimann, W. (2015). On Mardia skewness and kurtosis of Soules basis matrices in ROM simulation. *Linear Algebra and its Applications*, 473:284–296.
- Joanes, D. and Gill, C. (1998). Comparing measures of sample skewness and kurtosis. *Journal of the Royal Statistical Society: Series D (The Statistician)*, 47(1):183–189.
- Kollo, T. (2008). Multivariate skewness and kurtosis measures with an application in ICA. *Journal of Multivariate Analysis*, 99(10):2328–2338.
- Ledermann, D. and Alexander, C. (2012). Further properties of random orthogonal matrix simulation. *Mathematics and Computers in Simulation*, 83:56–79.

- Ledermann, W., Alexander, C., and Ledermann, D. (2011). Random orthogonal matrix simulation. *Linear Algebra and its Applications*, 434(6):1444–1467.
- Lyon, A., Mincholé, A., Martínez, J. P., Laguna, P., and Rodriguez, B. (2018). Computational techniques for ecg analysis and interpretation in light of their contribution to medical advances. *Journal of The Royal Society Interface*, 15(138):20170821.
- Ma, J. and He, P. (2016). Fast Monte Carlo simulation for pricing covariance swap under correlated stochastic volatility models. *IAENG International Journal of Applied Mathematics*, 46(3):336–345.
- Mardia, K. V. (1970). Measures of multivariate skewness and kurtosis with applications. *Biometrika*, 57(3):519–530.
- McSharry, P. E., Clifford, G. D., Tarassenko, L., and Smith, L. A. (2003). A dynamical model for generating synthetic electrocardiogram signals. *IEEE Transactions on Biomedical Engineering*, 50(3):289–294.
- Oberkampf, W. L., DeLand, S. M., Rutherford, B. M., Diegert, K. V., and Alvin, K. F. (2002). Error and uncertainty in modeling and simulation. *Reliability Engineering & System Safety*, 75(3):333–357.
- Quintana, C., Millwater, H., Singh, G., and Golden, P. (2015). Optimal allocation of testing resources for statistical simulations. *Engineering Optimization*, 47(7):979–993.
- Saliby, E. and Paul, R. (2009). A farewell to the use of antithetic variates in Monte Carlo simulation. *Journal of the Operational Research Society*, 60(7):1026–1035.
- Swain, J. and Schmeiser, B. (1988). Control variates for Monte Carlo analysis of nonlinear statistical models, II: raw moments and variances. *Journal of Statistical Computation and Simulation*, 30(1):39–56.
- Szántai, T. (2000). Improved bounds and simulation procedures on the value of the multivariate normal probability distribution function. *Annals of Operations Research*, 100:85–101.
- Takanami, T. and Kitagawa, G. (1991). Estimation of the arrival times of seismic waves by multivariate time series model. *Annals of the Institute of Statistical Mathematics*, 43(3):407–433.
- Thomopoulos, N. T. (2012). *Essentials of Monte Carlo Simulation: Statistical Methods for Building Simulation Models*. Springer Science & Business Media.

## Appendix

### A Theoretical proofs

*Proof of Lemma 1.* For convenience, let us re-write the system (18-1)–(18-3) as follows:

$$\begin{aligned}
 s_{11} + s_{21} + s_{31} &= - \sum_{i=4}^m w_{i1} =: a, \\
 s_{11}^2 + s_{21}^2 + s_{31}^2 &= m - \sum_{i=4}^m w_{i1}^2 =: b, \\
 s_{11}^3 + s_{21}^3 + s_{31}^3 &= mp_1 - \sum_{i=4}^m w_{i1}^3 =: c.
 \end{aligned}$$

Let  $x_1 = s_{11} - \frac{a}{3}$ ,  $x_2 = s_{21} - \frac{a}{3}$  and  $x_3 = s_{31} - \frac{a}{3}$ . Then, the above equations reduce to:

$$x_1 + x_2 + x_3 = 0, \quad (\text{A.1})$$

$$x_1^2 + x_2^2 + x_3^2 = b - \frac{a^2}{3} =: d, \quad (\text{A.2})$$

$$x_1^3 + x_2^3 + x_3^3 = c - ab + \frac{9}{2}a^3 =: e. \quad (\text{A.3})$$

We want to establish the conditions under which the system of equations has real roots. After eliminating  $x_2$  and  $x_3$ , we obtain

$$6x_1^3 - 3dx_1 - 2e = 0. \quad (\text{A.4})$$

This is a cubic equation for  $x_1$  and always has a real root of the form  $x_1^* = \sqrt[3]{\frac{e}{6} + \sqrt{\Delta_3}} + \sqrt[3]{\frac{e}{6} - \sqrt{\Delta_3}}$ , where  $\Delta_3 = (e/6)^2 - (d/6)^3$  (Cardano, 1968). Substitute  $x_1^*$  in equation (A.1) and equation (A.2). Then we get a quadratic equation for  $x_2$ ,

$$x_2^2 + x_1^*x_2 + x_1^{*2} - \frac{d}{2} = 0. \quad (\text{A.5})$$

By the simple linear equation (A.1), it is sufficient to analyse when the quadratic equation (A.5) has a real root. Using a standard result for quadratic equations, equation (A.5) has a real root if and only if the following discriminant is non-negative,

$$\Delta_2 = x_1^{*2} - 4 \times \left(x_1^{*2} - \frac{1}{2}d\right) = 2d - 3x_1^{*2}$$

After some tedious algebra, the discriminant  $\Delta_2$  can be simplified as follows:

$$\Delta_2 = 2d - 3x_1^{*2} = -3 \left(x_1^{*2} - \frac{2}{3}d\right) = -3 \left(\sqrt[3]{\frac{e}{6} + \sqrt{\Delta_3}} - \sqrt[3]{\frac{e}{6} - \sqrt{\Delta_3}}\right)^2.$$

Now we can see that  $\Delta_2 \geq 0$  if and only if  $\Delta_3 \leq 0$ :

(i) When  $\Delta_3 = 0$ ,  $\Delta_2 = -3 \left(\sqrt[3]{\frac{e}{6}} - \sqrt[3]{\frac{e}{6}}\right)^2 = 0$ ;

(ii) When  $\Delta_3 > 0$ ,  $\Delta_2 = -3 \left(\sqrt[3]{\frac{e}{6} + \sqrt{\Delta_3}} - \sqrt[3]{\frac{e}{6} - \sqrt{\Delta_3}}\right)^2 < 0$ ;

(iii) When  $\Delta_3 < 0$ , there are three distinct real roots for (A.4), which may be expressed in terms of polar coordinates  $\cos \alpha \pm i \sin \alpha$ , where  $\alpha = \arccos \frac{e}{6R}$  and  $R^2 = \left(\frac{e}{6}\right)^2 - \Delta_3 = \left(\frac{d}{6}\right)^3$ . So, after some algebra,  $\Delta_2$  may be written:

$$\Delta_2 = -3 \left(\sqrt[3]{\frac{e}{6} + i\sqrt{-\Delta_3}} - \sqrt[3]{\frac{e}{6} - i\sqrt{-\Delta_3}}\right)^2 = 2d \sin^2 \frac{\alpha}{3} > 0.$$

Recall that  $\Delta_3 = (e/6)^2 - (d/6)^3$ , hence, the necessary and sufficient condition for equation (A.5) to have a real root is  $\Delta_3 \leq 0$ , viz.  $d^3 \geq 6e^2$ . The proof is complete.  $\square$

*Proof of Theorem 1 (ii) and (iii).* Here we establish the necessary and sufficient conditions for the system (17-1)-(17-4) to be solvable when  $k = 1, \dots, n$ . The system can be expressed in matrix form, as in equations (20) and (21), i.e.  $\mathbf{U}\mathbf{y} = \mathbf{v}$  and  $\mathbf{y}'\mathbf{y} = m - \sum_{i=k+3}^m w_{ik}^2$ . First, it is easy to see that condition (ii) is a necessary and sufficient condition for the linear equation (20) to be solvable, i.e.  $\text{Rank}(\mathbf{U}) = \text{Rank}([\mathbf{U}, \mathbf{v}])$  where  $[\mathbf{U}, \mathbf{v}]$  is the augmented matrix. Next we need to focus on the quadratic equation (21). The idea is to use the linear equation (20) to identify a set of linearly independent columns  $\mathbf{U}_1$  of  $\mathbf{U}$  with full column rank, which enables us to express the rest columns  $\mathbf{U}_2$  as a linear combination of  $\mathbf{U}_1$ , then the quadratic equation (21) becomes an equation on  $\mathbf{U}_1$ . More specifically, re-write equation (20) using  $\mathbf{U}_1$  and  $\mathbf{U}_2$  as  $\mathbf{U}_1\mathbf{y}_1 + \mathbf{U}_2\mathbf{y}_2 = \mathbf{v}$ , where the vectors  $\mathbf{y}_1$  and  $\mathbf{y}_2$  contain the elements in  $\mathbf{y}$  that correspond to  $\mathbf{U}_1$  and  $\mathbf{U}_2$  respectively. Therefore, we could eliminate  $\mathbf{y}_1$  in equation (21) by  $\mathbf{y}_1 = \mathbf{U}_1^+ (\mathbf{v} - \mathbf{U}_2\mathbf{y}_2)$ , where  $\mathbf{U}_1^+ = (\mathbf{U}_1'\mathbf{U}_1)^{-1} \mathbf{U}_1'$  is a Moore-Penrose inverse of  $\mathbf{U}_1$  (Golub and Van Loan, 2012). The Moore-Penrose inverse is in fact unique in this case, as  $\mathbf{U}_1$  has the full column rank  $\mathbf{U}_1$  of  $\mathbf{U}$ . Then the quadratic equation (21) becomes

$$\mathbf{y}_2'\mathbf{G}\mathbf{y}_2 - 2\mathbf{y}_2'\mathbf{g} + \mathbf{v}'(\mathbf{U}_1\mathbf{U}_1')^+\mathbf{v} + \sum_{j=i+3}^m w_{ji}^2 - m = 0. \quad (\text{A.6})$$

where  $\mathbf{G} = \mathbf{I} + \mathbf{U}_2'(\mathbf{U}_1\mathbf{U}_1')^+\mathbf{U}_2$  and  $\mathbf{g} = \mathbf{U}_2'(\mathbf{U}_1\mathbf{U}_1')^+\mathbf{v}$ . After completing the square, equation (A.6) becomes:

$$\mathbf{z}'\mathbf{G}\mathbf{z} = \mathbf{g}'\mathbf{G}^{-1}\mathbf{g} - \mathbf{v}'(\mathbf{U}_1\mathbf{U}_1')^+\mathbf{v} - \sum_{j=i+3}^m w_{ji}^2 + m,$$

where  $\mathbf{z} = \mathbf{y}_2 - \mathbf{G}^{-1}\mathbf{g}$ . Notice that  $\mathbf{G}$  is a positive-definite matrix, hence to ensure real roots of the above equation the right side of the equation must be non-negative. Therefore we obtain the condition (iii), viz.

$$\mathbf{g}'\mathbf{G}^{-1}\mathbf{g} - \mathbf{v}'(\mathbf{U}_1\mathbf{U}_1')^+\mathbf{v} \geq \sum_{j=i+3}^m w_{ji}^2 - m.$$

□

*Proof of Corollary 1.* We show that the zero arbitrary values are admissible under very mild conditions. In fact, they are not admissible only in the highly unusual cases where the number of simulations is very small and there exists one element of the Kollo skewness vector with large magnitude. To proceed, we check whether the system (17-1)-(17-4) satisfy the conditions in use Theorem 1, column by column, when all arbitrary values are zero. When  $k = 1$  we just need to check whether zero arbitrary values satisfy condition Theorem 1 (i). In this case, we have

$$a = -\sum_{i=4}^m w_{i1} = 0, b = m - \sum_{i=4}^m w_{i1}^2 = m, \text{ and } c = mp_1 - \sum_{i=4}^m w_{i1}^3 = mp_1.$$

Then the equation (19) becomes:

$$(b - \frac{a^2}{3})^3 \geq 6(c - ab + \frac{9}{2}a^3)^2 \Leftrightarrow b^3 \geq 6c^2 \Leftrightarrow m^3 \geq 6m^2p_1^2 \Leftrightarrow p_1^2 \leq \frac{m}{6}. \quad (\text{A.7})$$

In practical applications,  $\frac{m}{6}$  is much larger than  $p_1^2$ , so equation (A.7) holds. For  $k = 2, \dots, n$  we need to check whether conditions Theorem 1 (ii)–(iii) are satisfied. Recall that in this case  $\mathbf{U}$  and  $\mathbf{v}$  become

$$\mathbf{U} = \begin{bmatrix} s_{11}^2 & s_{21}^2 & s_{31}^2 & 0 & 0 & \dots & 0 & 0 \\ s_{11} & s_{21} & s_{31} & 0 & 0 & \dots & 0 & 0 \\ s_{12} & s_{22} & s_{32} & s_{42} & 0 & \dots & 0 & 0 \\ \vdots & \vdots \\ s_{1,k-1} & s_{2,k-1} & s_{3,k-1} & s_{4,k-1} & s_{5,k-1} & \dots & s_{k+1,k-1} & 0 \\ 1 & 1 & 1 & 1 & 1 & \dots & 1 & 1 \end{bmatrix}, \quad \mathbf{v} = \begin{bmatrix} mp_k \\ 0 \\ 0 \\ \dots \\ 0 \\ 0 \end{bmatrix}.$$

Let  $\mathbf{U}_1$  be the the matrix consisting of the first  $k + 1$  columns of  $\mathbf{U}$ , then we can compute the determinant of  $\mathbf{U}_1 \mathbf{U}_1'$  as:

$$\det(\mathbf{U}_1 \mathbf{U}_1') = t(k + 1)m^{k-1},$$

where  $t = s_{11}^4 + s_{21}^4 + s_{31}^4 - m \left( \frac{m}{k+1} + p_1^2 + \dots + p_{k-1}^2 \right)$ . As  $t > 0$  by assumption, we get that  $\mathbf{U}_1$  is invertible, hence is of full row rank, which implies that  $\mathbf{v}$  must be in the span of  $\mathbf{U}_1$ . Hence Theorem 1 (ii) holds.

If the system has real solutions, the condition (iii) requires  $\mathbf{g}' \mathbf{G}^{-1} \mathbf{g} - \mathbf{v}' \left( \mathbf{U}_1 \mathbf{U}_1' \right)^+ \mathbf{v} \geq -m$ . After some algebraic computation, we get

$$\mathbf{v}' \left( \mathbf{U}_1 \mathbf{U}_1' \right)^+ \mathbf{v} = \frac{m^2 p_k^2}{t}, \quad \mathbf{G} = 1 + \frac{1}{k+1} + \frac{1}{t} \left( \frac{m}{k+1} \right)^2, \quad \mathbf{g} = -\frac{m^2 p_k}{t(k+1)},$$

and condition (iii) becomes  $\frac{t}{m} + \frac{m}{(k+1)(k+1)} \geq p_k^2$ . In practical applications,  $m$  is much larger than  $n$  and  $k \leq n$ , so this inequality always holds. Thus the proof is complete. To summarise, setting all arbitrary values to zero is admissible under very mild conditions.  $\square$

## B Further results on normal arbitrary values

Here we discuss the theoretical failure rate for the first column of  $\mathbf{S}_{mn}$ , that is  $\mathbf{s}_1 = [s_{11}, \dots, s_{m1}]'$ , when using normal arbitrary values  $s_{i1} = w_{i1}$  for  $i = 4, \dots, m$  which are drawn from  $\mathcal{N}(0, \sigma^2)$  with the mean and variance adjustment given by equation (23). This way, the arbitrary variables should follow i.i.d.  $\mathcal{N}(0, \sigma^2)$ , and we can denote these  $m - 3$  random variables  $[W_{41}, W_{51}, \dots, W_{m1}]'$ . We can calculate auxiliary variables corresponding to their first three moments:

$$\begin{aligned} M_1 &= \frac{1}{m-3} \sum_{i=4}^n (W_{i1}) = \frac{1}{m-3} \sum_{i=4}^n \left( \frac{\sigma}{s_z} (Z_j - \bar{Z}) \right) = 0 \\ M_2 &= \frac{1}{m-3} \sum_{i=4}^n (W_{i1} - M_1)^2 = \frac{1}{m-3} \sum_{i=4}^n \left( \frac{\sigma}{s_z} (Z_j - \bar{Z}) \right)^2 = \sigma^2 \\ M_3 &= \frac{1}{m-3} \sum_{i=4}^n (W_{i1} - M_1)^3 = \frac{1}{m-3} \sum_{i=4}^n \left( \frac{\sigma}{s_z} (Z_j - \bar{Z}) \right)^3 = \frac{\sum_{i=4}^n (Z_j - \bar{Z})^3}{(m-3)s_z^3} \sigma^3 \end{aligned}$$

Note that  $M_1$  and  $M_2$  are both constants, taking the values 0 and  $\sigma^2$  respectively.

By the central limit theorem (Joanes and Gill, 1998) when the simulation sample size  $m$  is large  $M_3$  has an approximate normal distribution with mean 0 and variance  $\frac{6(m-5)}{m(m-2)}\sigma^6$ . Therefore, for any arbitrary values selected this way, we have:

$$\sum_{i=4}^m w_{i1} = 0, \sum_{i=4}^m w_{i1}^2 = (m-3)\sigma^2, \sum_{i=4}^m w_{i1}^3 = (m-3)M_3.$$

Next we check Lemma 1 for  $[W_{41}, W_{51}, \dots, W_{m1}]'$  to see whether they are admissible. Since  $a = 0$ ,  $b = m - (m-3)\sigma^2$  and  $c = mp_1 - (m-3)M_3$  in equation (19) we can rewrite the condition as:

$$p_1q - \sqrt{\frac{m-3}{6}(q-\sigma^2)^3} \leq M_3 \leq p_1q + \sqrt{\frac{m-3}{6}(q-\sigma^2)^3} \quad (\text{B.1})$$

where  $q = \frac{m}{m-3}$ . So the probability of  $[W_{41}, W_{51}, \dots, W_{m1}]'$  being admissible is the probability of  $M_3$  lying within the range given by (B.1).

Let  $h(\sigma)$  denote the failure rate for the arbitrary values, i.e. the probability that the arbitrary values do not satisfy the condition (B.1). When  $\sigma = 0$ ,  $[W_{41}, W_{51}, \dots, W_{m1}]'$  are essentially zero. By Corollary 1 zero arbitrary values are always admissible when  $p_1^2 \leq \frac{m}{6}$ , hence we have  $h(0) = 0$ . When  $\sigma \neq 0$ , because  $M_3$  is approximately normal distributed with mean 0 and variance  $\frac{6(m-5)}{m(m-2)}\sigma^6$ , let  $\Phi(\cdot)$  and  $\varphi(\cdot)$  denote the cumulative distribution function and probability density function for a standard normal distribution, then we have

$$h(\sigma) = 1 - (\Phi(I_U) - \Phi(I_L)) \quad \text{for } 0 < \sigma \leq \sqrt{q} \quad (\text{B.2})$$

where  $I_U = \frac{1}{\sigma^3} \sqrt{\frac{m(m-2)}{6(m-5)}} \left( p_1q + \sqrt{\frac{m-3}{6}(q-\sigma^2)^3} \right)$  and  $I_L = \frac{1}{\sigma^3} \sqrt{\frac{m(m-2)}{6(m-5)}} \left( p_1q - \sqrt{\frac{m-3}{6}(q-\sigma^2)^3} \right)$ .

## C Algorithms

The HPSW algorithm by Hanke et al. (2017) is summarized as follows:

---

### Algorithm 1 HPSW by (Hanke et al., 2017)

---

```

1: function GETM_1( $m, \tau$ )                                 $\triangleright m$ : the number of observations,  $\tau$ : target Kollo skewness
2:    $n = \text{length}(\tau)$ 
3:   generate  $\mathbf{\Omega}_n$                                         $\triangleright n \times n$  matrix with  $\mathbf{1}'_n \mathbf{\Omega}_n = (\sqrt{n}, 0, \dots, 0)$ 
4:    $\mathbf{p}_n = \mathbf{\Omega}_n^{-1} n^{-1} \tau$ 
5:   for  $k = 1, \dots, n$  do
6:     set arbitrary values for elements  $\{s_{k+3k}, \dots, s_{mk}\}$ 
7:     solve (17-1) to (17-4) and get elements  $\{s_{1k}, \dots, s_{k+2k}\}$ 
8:    $\mathbf{M}_{mn} = \mathbf{S}_{mn} \mathbf{\Omega}'_n$                                  $\triangleright$  rotate back
9:   return  $\mathbf{M}_{mn}$ 

```

---

We modify the HPSW algorithm using our necessary and sufficient conditions on arbitrary values in each column of  $\mathbf{S}_{mn}$  derived in Theorem 1. We check these conditions before solving the equations (17-1) – (17-4) and regenerate arbitrary values until our conditions are satisfied. Additionally we

extend the algorithm by proposing some novel ways to generate arbitrary values and adjust them via equation (23) so they are more likely to be admissible. The modified and extended HPSW algorithm is shown below:

---

**Algorithm 2** Modified and extended HPSW algorithm

---

```

1: function GETM_2( $m, \tau$ )                                     ▷  $m$ : the number of observations,  $\tau$ : target Kollo skewness
2:    $n = \text{length}(\tau)$ 
3:   generate  $\Omega_n$                                            ▷  $n \times n$  matrix with  $\mathbf{1}'_n \Omega_n = (\sqrt{n}, 0, \dots, 0)$ 
4:    $\mathbf{p}_n = \Omega_n^{-1} n^{-1} \tau$ 
5:   while Lemma 1 does not hold do                             ▷ solve for the first column
6:     generate random values  $\{z_{41}, \dots, z_{m1}\}$  by bootstrapping or from a distribution
7:     obtain arbitrary value  $\{w_{41}, \dots, w_{m1}\}$  from  $z_{i1}$  by (23) and check Lemma 1
8:     if Lemma 1 holds then
9:       fill  $\{s_{41}, \dots, s_{m1}\}$  with  $\{w_{41}, \dots, w_{m1}\}$ 
10:    solve (17-1) to (17-4) for elements  $\{s_{11}, \dots, s_{31}\}$ 
11:    for  $k = 2, \dots, n$  do                                   ▷ solve for the rest column by column
12:      while Theorem 1(ii)(iii) are not satisfied do
13:        generate random values  $\{z_{k+3k}, \dots, z_{mk}\}$  by bootstrapping or from a distribution
14:        obtain arbitrary values  $\{w_{k+3k}, \dots, w_{mk}\}$  by (23) and check Theorem 1 (ii)(iii)
15:        if Theorem 1 (ii)(iii) hold then
16:          fill  $\{s_{k+3k}, \dots, s_{mk}\}$  with  $\{w_{k+3k}, \dots, w_{mk}\}$ 
17:        solve (17-1) to (17-4) to obtain elements  $\{s_{1k}, \dots, s_{k+2k}\}$ 
18:       $\mathbf{M}_{mn} = \mathbf{S}_{mn} \Omega'_n$                                ▷ rotate back to get  $\mathbf{M}_{mn}$ 
19:    return  $\mathbf{M}_{mn}$ 

```

---

The pseudo-code for concatenated HPSW (CHPSW) algorithm described in Section 3.3 is applied on each sub-sample as follows:

---

**Algorithm 3** CHPSW algorithm

---

```

1: function GETCM( $m, \tau, N$ )                                   ▷  $N$ : the number of subsamples to concatenate
2:    $n = \text{length}(\tau)$ 
3:   generate  $\Omega_n$                                            ▷  $n \times n$  matrix with  $\mathbf{1}'_n \Omega_n = (\sqrt{n}, 0, \dots, 0)$ 
4:    $\mathbf{p}_n = \Omega_n^{-1} n^{-1} \tau$ 
5:    $l = \max\{n + 2, \lfloor \frac{m}{N} \rfloor\}$                              ▷  $\lfloor x \rfloor$  returns the greatest integer less than or equal to  $x$ 
6:   for  $k = 1, \dots, N - 1$  do                                 ▷ obtain the first  $N - 1$  subsamples with length  $l$ 
7:      $\mathbf{M}_{(kl-k+1):kl, n} = \text{GETM\_2}(l, \tau)$ 
8:    $\mathbf{M}_{(Nl-l+1):m, n} = \text{GETM\_2}(m - Nl - l, \tau)$            ▷ obtain the last sub-samples with length  $m - l(N - 1)$ 
9:   return  $\mathbf{M}_{mn}$ 

```

---

Finally, we specify the matrix  $\mathbf{\Omega}_n$  used for all ROM simulations in Section 4:

$$\begin{pmatrix} \frac{1}{\sqrt{n}} & \frac{(-1)^{n-1}}{\sqrt{n/(n-1)}} & 0 & 0 & \cdots & 0 & 0 & 0 \\ \frac{1}{\sqrt{n}} & \frac{(-1)^n}{\sqrt{n(n-1)}} & \frac{(-1)^{n-1}}{\sqrt{(n-1)/(n-2)}} & 0 & \cdots & 0 & 0 & 0 \\ \frac{1}{\sqrt{n}} & \frac{(-1)^n}{\sqrt{n(n-1)}} & \frac{(-1)^n}{\sqrt{(n-1)(n-2)}} & \frac{(-1)^{n-1}}{\sqrt{(n-2)/(n-3)}} & \cdots & 0 & 0 & 0 \\ \frac{1}{\sqrt{n}} & \frac{(-1)^n}{\sqrt{n(n-1)}} & \frac{(-1)^n}{\sqrt{(n-1)(n-2)}} & \frac{(-1)^n}{\sqrt{(n-2)(n-3)}} & \cdots & 0 & 0 & 0 \\ \vdots & \vdots \\ \frac{1}{\sqrt{n}} & \frac{(-1)^n}{\sqrt{n(n-1)}} & \frac{(-1)^n}{\sqrt{(n-1)(n-2)}} & \frac{(-1)^n}{\sqrt{(n-2)(n-3)}} & \cdots & \frac{(-1)^n}{\sqrt{4 \times 3}} & \frac{(-1)^{n-1}}{\sqrt{3/2}} & 0 \\ \frac{1}{\sqrt{n}} & \frac{(-1)^n}{\sqrt{n(n-1)}} & \frac{(-1)^n}{\sqrt{(n-1)(n-2)}} & \frac{(-1)^n}{\sqrt{(n-2)(n-3)}} & \cdots & \frac{(-1)^n}{\sqrt{4 \times 3}} & \frac{(-1)^n}{\sqrt{3 \times 2}} & \frac{(-1)^{n-1}}{\sqrt{2}} \\ \frac{1}{\sqrt{n}} & \frac{(-1)^n}{\sqrt{n(n-1)}} & \frac{(-1)^n}{\sqrt{(n-1)(n-2)}} & \frac{(-1)^n}{\sqrt{(n-2)(n-3)}} & \cdots & \frac{(-1)^n}{\sqrt{4 \times 3}} & \frac{(-1)^n}{\sqrt{3 \times 2}} & \frac{(-1)^n}{\sqrt{2}} \end{pmatrix}.$$